Plant-microbe-mediated decrease of greenhouse gases under dynamic wetland hydrology

Regina B. Bledsoe, Colin G. Finlay, Ariane L. Peralta*

Department of Biology, East Carolina University, Greenville, NC 27858, USA;

*Corresponding author: telephone: +1 252.328.2712, e-mail: peraltaa@ecu.edu

Abstract

While wetlands represent a small fraction (~5-10%) of the world's land surface, it is estimated that one third of wetlands have been lost due to human activities. Wetland habitat loss decreases ecosystem benefits such as improving water quality and mitigating climate change. These microbially mediated functions are dependent on redox conditions, which are altered by soil hydrology and the presence of plants. In this study, we hypothesized that redox status due to continuous flooding would support greater abundance of microbial taxa involved in methanogenesis (obligate anaerobes), but plant-mediated oxygen transport would decrease methane emissions. Using a mesocosm design, we manipulated the duration of hydrologic conditions (i.e., stable dry, stable flooding, and alternating wet/dry) and presence of plants to induce soil redox changes in wetland soils. We measured soil redox status, used targeted amplicon and shotgun metagenomic sequencing to characterize microbial communities, and measured greenhouse gas production to assess microbial function. Results showed that hydrologic history influenced microbial community composition while plant presence and hydrologic treatment altered microbial functional gene composition to a lesser degree. Plant presence decreased greenhouse gas production while differences in the community composition of functional genes related to carbohydrate metabolism, denitrification, and methanogenesis also explained variation in emissions of carbon dioxide and to a lesser extent, methane. While previous studies do not often include plants when assessing greenhouse gas emissions, this study highlights that plant-mediated decreases in greenhouse gas emissions are important and plant-mediated effects should be considered when estimating the carbon balance of ecosystems.

Importance

This study revealed that initial hydrologic conditions (compared to manipulated hydrology) strongly influenced microbial community composition more than function. Specifically, results showed that hydrology is a strong environmental filter that determines microbial taxonomic and functional community patterns, short-term redox changes that are most distinct from historic redox conditions shift microbial communities, and plant presence can stabilize redox shifts and mediate greenhouse gas production. These results support the importance of considering plant presence/absence, and the duration of flooding and drying periods in wetland greenhouse gas production.

60 **Introduction**

61 Wetlands represent only 5-10% of terrestrial land surface (Kingsford et al. 2016) (1);
62 however, it is estimated that we have lost at least 21% of wetlands as of 2023 (2). Loss of
63 important functions is a consequence of land use conversion of wetlands to urban and
64 agricultural development. These wetland ecosystems provide valuable services such as
65 improving water quality by decreasing nutrient and pollutant loads and mitigating climate change
66 by sequestering carbon. Therefore, there is an interest in conserving, restoring, and
67 constructing wetlands for these ecosystem benefits. Examples of valuable wetland ecosystem
68 functions are anaerobic microbial processes associated with saturated soils that promote
69 complete inorganic nitrogen removal via denitrification ($NO_3^- \rightarrow N_2$) and suppress aerobic
70 decomposition of organic matter. These same anoxic soil conditions can also support methane
71 production (via methanogenesis), which could decrease long-term carbon storage and climate
72 change mitigation benefits of wetlands. Microbial functions associated with delivery of
73 ecosystem services have the potential to be managed to enhance beneficial wetland services
74 (3). To achieve microbial management, a deeper understanding of the controls on wetland
75 microbial ecosystem functions is needed.

76 To produce cellular energy, adenosine triphosphate (ATP), microorganisms catalyze a
77 series of oxidation-reduction (redox) reactions. Aerobic respiration yields the greatest amount of
78 energy and is expected under dry conditions but as water fills soil pore spaces, the soil matrix
79 shifts to a reducing environment (4, 5). Reducing environments favor anaerobic respiration in
80 which other molecules such as nitrate, manganese, ferric iron, sulfate, and carbon dioxide are
81 used as terminal electron acceptors (6). As soil moisture increases, oxygen availability and soil
82 redox potentials decrease , which corresponds to a shift in available electron acceptors (5).
83 Redox potentials measured between +600 and + 250 mV are considered oxidative conditions
84 while redox potentials measured from +250 to -400 mV are considered reducing conditions (5).

Therefore, measuring soil redox potential is useful for predicting which biogeochemical processes are likely to be carried out by soil microbes.

In order to manage microbial functions in support of nitrogen removal and retention but with decreased methane production, a better understanding of the extent that the presence of vegetation and changes in hydrology (e.g., flooding, drying) affect microbial communities is needed. Complex interactions between abiotic factors, such as soil physicochemical properties, redox status and nutrient availability, and biotic factors, including abundance of vegetation and microbial community structure, influence microbial functions to varying degrees. A microbial community is composed of many taxa with varying physiologies which respond differently to changes in the local environment (7, 8). Particular microbes may be more adapted to specific hydrologic conditions in their environment, where only a subset of microbial taxa can persist in response to frequent changes in soil moisture (5, 9). However, unexpected microbial responses can also occur due to dormancy of soil bacterial taxa (10, 11). As such, hydrologic changes in wetlands due to drought, draining, and re-wetting cause shifts in soil redox potentials and microbial community composition and metabolism, which can influence the relative rates of anaerobic processes such as denitrification and methanogenesis (5, 9, 12).

If drying and re-wetting events are periodic, a cycle of activity and dormancy can maintain high microbial diversity compared to more stable environmental conditions (9). For example, denitrifiers are facultative anaerobes and are capable of using oxygen; but in anoxic conditions, denitrifiers can switch to reducing nitrate (NO_3^-) to nitrous oxide (N_2O) and dinitrogen (N_2) gas during respiration (13). In addition, methanogens are dominant in the most anoxic conditions such as flooded wetlands, and are responsible for converting carbon dioxide to methane gas (13). Fluctuating hydrologic conditions can shift the microbial community to one that can only tolerate transitional zones. As hydrologic changes occur, anoxic-oxic interfaces provide environmental conditions that sometimes support methanotrophs that convert methane to carbon dioxide and denitrifiers (13–15). Therefore, the availability of electron acceptors (e.g.,

oxygen, nitrate) in the soil environment influences the relative abundance of microbial functional groups (i.e., subset of microbes capable of using a suite of electron acceptors) and rates and types of microbial processes.

While hydrology is a primary determinant of soil redox potential, plants also modify the soil environment. The soil microenvironments that are in contact with plant roots are hotspots of microbial activity involved in transporting nutrients, oxygen, and carbon belowground (16–18). Plants can also transport methane aboveground through aerenchyma in shoots. Also, radial oxygen loss from plant roots can increase soil redox potentials around the root zone producing microenvironments that can support aerobic microbial processes (18). Additionally, vegetation can alter soil redox potentials by facilitating transport of oxygen into roots zones (18, 19) and transporting methane from root zones into the atmosphere (20, 21).

The aim of this study is to provide insight into how the duration of hydrologic change (i.e., dry, interim, wet), and the presence of vegetation in wetland soils change the structure of the microbial community, redox conditions, and greenhouse gas rates. We hypothesize that dry and dry/wet transition conditions will support similar microbial communities, but that redox potentials and greenhouse gas rates will differ between manipulated hydrologic treatment conditions. We expect that dry conditions with and without vegetation will support higher redox potentials (i.e., oxidative conditions) and a higher rate of carbon dioxide production with some nitrous oxide production but little or no methane production. We expect this because dry and transition conditions should support similar communities of facultative anaerobes that can switch between respiration pathways depending on current soil saturation levels. Additionally, in dry conditions soils are already aerated so plant-mediated gas transport belowground should not alter redox potentials. However, in fluctuating wet conditions, we expect that redox conditions will shift between oxidative and reducing conditions due to soil saturation. Also, the plant presence will increase redox potentials during saturated periods, due to plant-mediated gas transport belowground, compared to treatments where vegetation is absent. Due to lower

oxygen levels when saturated conditions are present, we expect decreased carbon dioxide production but increased nitrous oxide production with plants and negative nitrous oxide rates without plants indicating incomplete or complete denitrification processes, respectively. Also, we expect methane production will be lower due to methanogens being obligate anaerobes. Flooded conditions will support different microbial communities than dry or fluctuating environments due to consistently low redox potentials (i.e., reducing conditions) resulting in the highest rates of methane production and complete denitrification rates since these are both anaerobic processes. Although, other studies (20, 21) have found increased methane rates in the presence of some plant species, in the present study, we expect that soils with plants will have lower methane production compared to flooded soils without plants. This is expected due to oxygen transport from roots supporting aerobic methanotrophic microbial taxa that consume methane.

To test these hypotheses, we conducted a mesocosm experiment in which we manipulated hydrology (i.e., dry, interim, and wet) and presence of plants in wetland soils collected from with different hydrologic histories (i.e., dry, wet/dry transition, and saturated wet zones) of a restored coastal plain wetland. We measured soil nutrient concentrations, redox potentials, greenhouse gas concentrations, and characterized soil microbial communities using amplicon sequencing. By simulating acute differences in hydrologic states, the addition of plants, and maintenance of soil structure, we were able to link microbial-scale changes to ecosystem-level processes.

Methods

Study site

We collected soil samples from the Timberlake Observatory for Wetland Restoration located in the Albemarle Peninsula in Tyrell County, North Carolina (35°54’22” N 76°09’25” W; Fig. 1). Previously described by (22) and(23), the field site is part of the Great Dismal Swamp

Mitigation Bank, LLC which is a 1,700 ha wetland consisting of 420 ha of mature forested wetland, 787 ha of forested wetland, 57.2 ha of drained shrub-scrub, and 440 ha of agricultural fields restored to wetland habitat in 2007 (22, 24). A major portion of the restoration effort was to remove drainage ditches and plant 750,000 saplings including *Taxodium distichum, Nyssa* spp., *Salix nigra, Fraxinus pennsylvanica, and Quercus* spp. (23). A more recent survey indicates that the dominant plant species at the site is *Juncus effusus* L. along with *Euthamia caroliniana* (L.) Greene ex Porter & Britton, *Solidago fistulosa* Mill., and *Scirpus cyperinus* (L.) Kunth (25). The site is connected to the Albemarle Sound via the Little Alligator River, and the site's position in the landscape increases the potential for saltwater intrusion to occur. In addition, salinity in the sound ranges from 0-7 psu and up to 12 psu during drought years (24). Even though there is little elevation change (-1 m to 2 m) across the restored wetland, there is a hydrologic gradient, which is driven by the position of the water table and represents upland dry, saturated wet, and transition dry/wet sites (25).

Mesocosm experimental design

We used a mesocosm approach to assess the changes in the soil microbial community, redox potentials, and greenhouse gas (GHG) production due to hydrologic changes and vegetation. We set up a mesocosm experiment using soil blocks collected from three sites within the Timberlake Observatory for Wetland Restoration field site. Soils were collected from the restored (12 years post-restoration) portion of the site that was previously used as agricultural fields for several decodes prior to restoration (22). We collected soils that represented three different hydrologic zones on the inflow side of the site at the following coordinates: 35°53'45.3"N 76°09'57.5"W (dry), 35°53'44.8"N 76°09'57.1"W (dry/wet transition or interim), and 35°53'44.3"N 76°09'56.0"W (wet). Six intact soil blocks (25 cm × 25 cm × 20 cm deep) were cut out from each of the three sites using landscaping knives and shovels. Soil history was determined by water table levels at the time of collection (dry = 20 cm, interim = 10

cm, and wet = 0 cm below surface level). Soil blocks were contained in dark plastic containers of the same dimensions as the soil blocks (Fig. 1). To manipulate hydrology within the mesocosm, vinyl tubing was inserted 3 cm from the bottom of the mesocosm container on each side and connected to a 1 L water bottle (Fig. 1). Water levels inside the mesocosm were maintained by filling the 1 L bottle to the desired height using rainwater collected from a cistern. To manipulate the presence of vegetation, the mesocosm was divided in half and separated by root screen (20 μm stainless steel mesh). On one side plants were allowed to grow during the experiment, while the 'no plant' side was maintained by careful removal of above- and belowground plant biomass. Finally, 4" schedule 40 polyvinyl chloride (PVC) collars were inserted 5 cm below the surface as a sampling base for GHG chambers (described in subsection *GHG concentrations*). The mesocosm experiment was housed at the East Carolina University West Research Campus (Greenville, NC) under a covered hoop house with shade cloth which prevented precipitation and allowed 60% light into the hoop house. Soils were collected April 1, 2016, prepared on May 29, 2016, and experimental mesocosm sampling started on June 13, 2016, and ended on August 11, 2016. Temperatures ranged from 22.7 °C ± 1.5 to 30.8 °C ± 1.4 during the experimental sampling period.

Two weeks after installing PVC collars and setting up the plant treatment, we started hydrologic treatments. Hydrologic manipulation occurred over eight weeks to allow for multiple dry/wet transitions for the interim treatment. Mesocosms exposed to wet conditions were flooded by overhead watering and maintained using water reservoirs filled to maximum container height (18 cm). Mesocosms exposed to dry conditions were maintained at a 5 cm water level. The dry/wet (interim) treatments fluctuated between flooded and dry conditions, as described above, every two weeks starting with a wet treatment and ending with a dry treatment. We measured soil redox status and microbial community composition at the beginning and end of the 8-week experiment. In addition, we measured GHG fluxes every two weeks starting two weeks after initiating hydrologic treatments. Finally, at the end of the eight-

week experiment, we collected soils for physiochemical analyses: soil moisture, pH, total carbon, total nitrogen, extractable ammonium and nitrate, phosphorus, potassium, magnesium, sulfur, iron, manganese, and organic matter concentrations (described in subsection *Soil Physiochemical Characteristics*).

Measuring integrated soil redox status

We measured soil redox status at the beginning and end of the hydrologic experiment using Indicator of Reduction in Soils (IRIS) tubes (InMass Technologies; (26) (Fig. S1A). The IRIS tubes are constructed from 1/2" schedule 40 PVC pipe coated in iron oxide (Fe (III)) paint (27). When exposed to oxidative conditions, Fe(III) is visible as an orange-red paint; but when exposed to anoxic conditions, Fe(III) is reduced to Fe(II) which dissolves in solution and appears as a clearing (white) on the tube (26, 27). At the beginning of the experiment, two IRIS tubes (12 cm depth) were installed in each mesocosm: one on the plant side and one on the bare soil side. The IRIS tubes were incubated in mesocosm conditions for two weeks before removal and analysis. After we removed the IRIS tube, a non-coated PVC pipe was used to fill the hole. Two weeks prior to the end of the experiment, the non-coated PVC pipe was removed and replaced with a new IRIS tube to measure soil redox status at the end of the experiment.

We quantified the surface area of Fe(III) paint removed from IRIS tubes using ImageJ software (v1.48, (28)). First, we imaged the entire tube by taking four pictures and then stitched the photo into a composite using GIMP2 (v2.8.14, https://gimp.org/) photo editing software. Next, we identified areas of artificial paint removal, that is scratches from installing or removing tubes, and manually filled these pixels. Then, using ImageJ software (v1.48, (28)), we converted all colored pixels to black. We compared the number of white pixels to total pixels to determine the percent of paint removed. Interpretation of redox status is based on the percent paint removed from a 10 cm section of tubing and summarized as follows: 0% not reducing, 1-5% probably not reducing, 5-10% possibly reducing, 10-25% and >25% definitely reducing (27).

Soil physiochemical characteristics

Soil proprieties were determined from soils collected during the destructive sampling of mesocosms at the end of the experimental duration. We collected six soil cores (3 cm diameter, 10 cm depth) from each side of the box (i.e., plant and no plant) and combined cores collected from one side into a composite sample (i.e., one plant composite and one no plant composite), passed soils through a 4 mm sieve, and homogenized samples prior to subsampling for soil analyses. For each sample, we measured gravimetric soil moisture by drying 20-30 g of field-moist soil at 105 °C for at least 24 hours. Approximately 5 g of field moist soil was extracted with 45 ml of 2 M KCl, and extractable ammonium (NH_4^+) and nitrate (NO_3^-) ions were colorimetrically measured using a SmartChem 200 auto analyzer (Unity Scientific Milford, Massachusetts, USA) at the East Carolina University Environmental Research Laboratory. To determine total carbon and total nitrogen (TC, TN), a subsample of air-dried soil was finely ground and sieved through a 500 µm mesh and analyzed using an elemental analyzer (2400 CHNS Analyzer; Perkin Elmer; Waltham, Massachusetts, USA) at the Environmental and Agricultural Testing Service Laboratory, Department of Crop and Soil Sciences, North Carolina State University. A second subsample of air-dried soil was sent to Waters Agricultural Laboratories, Inc. (Warsaw, NC) and analyzed for pH, phosphorus, potassium, magnesium, sulfur, manganese, iron, and humic matter, using standard Mehlich III methods (29, 30).

Greenhouse gas (GHG) concentrations

We examined the effects of hydrology and vegetation on GHG production. We measured GHG concentrations on June 13, 2016, two weeks after hydrologic treatments were established, and then every two weeks until August 11, 2016, for a total of five sampling events. The GHG collection chambers were 20 cm in height with a diameter of 8.25 cm and constructed from clear acrylic tubing. Since GHG samples were captured using clear chambers versus opaque

267 chambers, GHG measurements represent total GHG fluxes and not just soil respiration due to
268 microbial activity. Chambers were sealed on one end with silicon and a pipe cap with 33 mm
269 septa installed as gas sampling port. At the time of sampling, chambers were placed on top of
270 preinstalled PVC collars and the seal taped to prevent diffusion from the seam (31). We
271 collected gas samples every 30 minutes for a total of four time points. To collect gas samples,
272 we used a needle attached to a 20 mL syringe, mixed headspace gas three times by pulling and
273 depressing the plunger, and then collected 20 mL of sample. The collected gas sample was
274 equally distributed between two 3 mL glass Exetainer vials (Lampeter, Wales, UK) fitted with
275 screw top and dual layer septa. Samples were stored upside down at room temperature in a
276 dark location and were analyzed within 96 hours of collection. We analyzed GHG
277 concentrations using a Shimazdu gas chromatograph (GC-2014) fitted with an electron capture
278 detector to detect nitrous oxide and flame ionization detector with methanizer to measure
279 methane and carbon dioxide. Calibration standards for June 13 and June 28, 2016 contained 0,
280 120, 240, 360, and 480 CO_2 ppm; 0, 1, 2, 3, 4, and 5 CH_4 ppm; 0, 0.2, 0.4, 0.6, 0.8, and 1 N_2O
281 ppm. Calibration standards for July 11, Jul 25, and August 11, 2016 contained 0, 120, 480,
282 1200, 2400, and 3000 CO_2 ppm; 0, 1, 4, 20, 40, and 50 CH_4 ppm; 0, 0.2, 0.8, 20, 40, and 50
283 N_2O ppm. If a sample measured above the calibration curve, we diluted the sample and
284 reanalyzed it.

285 We used the linear change in concentration and the ideal gas law to calculate GHG
286 fluxes (32). However, upon curation of analyzed gas samples for GHG flux calculations, we
287 identified that 30-50% of samples from no plant treatments were not linear and that 50-75% of
288 those samples represented wet treatments. Due to the statistical power lost in determining the
289 effects of hydrology and plants on GHG rates by removing these samples from further analyses,
290 we chose an alternate approach to analyzing gas samples. We determined the concentration of
291 CH_4, CO_2, and N_2O in each sample for the first sampling time point which occurred at the first
292 30-minute collection interval.

Bacterial and archaeal community analyses

We assessed the soil microbial community composition at the beginning of the experiment ('start' based on soils collected from the IRIS tube installation) and at the end of the experiment ('final' based on soils collected during destructive sampling). We collected 'final' soil samples using a standard soil probe (3 cm diameter, 10 cm deep) from the same location that we collected GHGs samples. We extracted genomic DNA from soils using the Qiagen DNeasy PowerSoil Kit and diluted DNA to 20 ng μl^{-1}. This genomic DNA was used as template in PCR reactions and used barcoded primers (bacterial/archaeal 515FB/806R primer set) originally developed by the Earth Microbiome Project (33) to target the V4 region of the bacterial 16S subunit of the ribosomal RNA gene (33–35). For each sample, three 50 µL PCR libraries were prepared by combining 35.75 µL molecular grade water, 5 µL Amplitaq Gold 360 10x buffer, 5 µL $MgCl_2$ (25 mM), 1 µL dNTPs (40mM total, 10mM each), 0.25 µL Amplitaq Gold 360 polymerase, 1 µL 515 forward barcoded primer (10 µM), 1 µL 806 reverse primer (10 µM), and 1 µL DNA template (10 ng μL^{-1}). Thermocycler conditions for PCR reactions were as follows: initial denaturation (94 °C, 3 minutes); 30 cycles of 94 °C for 45 seconds, 50 °C for 30 seconds, 72 °C for 90 seconds; final elongation (72 °C, 10 minutes). The triplicate 50 µL PCR libraries were combined and then cleaned using the Axygen® AxyPrep Magnetic (MAG) Bead Purification Kit (Axygen, Union City, California, USA). Cleaned PCR product were quantified using QuantIT dsDNA BR assay (Thermo Scientific, Waltham, Massachusetts, USA) and diluted to a concentration of 10 ng μL^{-1} before pooling libraries in equimolar concentration of 5 ng μL^{-1}. We sequenced the pooled libraries using the Illumina MiSeq platform using paired end reads (Illumina Reagent Kit v2, 500 reaction kit) at the Indiana University Center for Genomics and Bioinformatics Sequencing Facility.

Sequences were processed using the mothur (v1.42.0) (36) MiSeq pipeline (37). We assembled contigs from the paired end reads, quality trimmed using a moving average quality

score (minimum quality score 35), aligned sequences to the SILVA rRNA database (v132) (38), and removed chimeric sequences using the VSEARCH algorithm (39). We created operational taxonomic units (OTUs) by first splitting sequences based on taxonomic class and then binning into OTUs based on 97% sequence similarity. Taxonomic identity was assigned using the SILVA rRNA database (v132) (38). Since amplicon sequencing was conducted using short-reads (250 bp) and not assembled genomes, we used an OTU-based 3% distance threshold to avoid splitting the same bacterial genome into distinct clusters (using amplicon sequence variant (ASV) of a single base difference). An OTU-based approach also limits over-inflated numbers of ASVs introduced by PCR bias and sequencing errors (40). In addition, employing an OTU- or ASV-based approach is known to result in similar broadscale community composition patterns (41).

Shotgun metagenomic analyses

Based on amplicon sequencing, we identified a subset of samples representing the most distinct microbial communities for shotgun metagenomic sequencing. Description of sample processing and metagenomic sequencing can be found in Peralta et al. (2020) (42). Briefly, we chose a set of baseline and post-flooding/drying treatment samples. We sourced mesocosm baseline conditions from relatively drier field locations (water level at about -20 cm, n=4) and relatively wetter plots (water level at about 0 cm, n=4). At the end of the 8-week experiment, we selected a subset of samples from the hydrologic treatments (prolonged drying or wetting only) and plant treatments (presence or absence of vegetation) (n = 16). After genomic DNA extraction using the Qiagen DNeasy PowerMax soil kit, samples were sent to the U.S. Department of Energy (DOE) Joint Genome Institute (JGI) for sequencing and analysis (GOLD study ID Gs0142547 and NCBI BioProject accession number PRJNA641216). Plate-based DNA library preparation and subsequent Illumina sequencing, according to published protocols (42),

resulted in 583.2 Gbp of raw sequence data. Raw data were processed using the DOE JGI Metagenome Annotation Pipeline IMG/M v.5.0.9 (43–45).

From the metagenomes, we curated functional gene sets using IMG/M's integrated Kyoto Encyclopedia of Genes and Genomes (KEGG) module list. For statistical analyses, we focused on the following four functional gene sets associated with biogenic greenhouse gas concentrations of N_2O, CH_4, and CO_2: (1) Denitrification (KEGG Module M00529), (2) Methanogen (M00617), (3) Central Carbohydrate Metabolism (M00001-M00011, M00307-M00309, M00580, and M00633), and (4) Prokaryotic Cytochrome C Oxidase (CcO) (M00155).

Statistical Analyses

All statistical analyses were performed in the R statistical environment (RStudio 2022.12.0+353, Rv4.2.2) (46). Prior to multivariate statistical analyses, we normalized sample-to-sample variation in sequence depth by taking the relative abundance of each OTU and dividing by the total number of OTUs for each soil community. We examined beta diversity by visualizing bacterial community responses to hydrologic history (field conditions), hydrologic treatment (contemporary dry/wet treatments), and plant presence/absence using principal coordinates analysis (PCoA) of bacterial community composition based on Bray-Curtis dissimilarity. We also used PCoA to visualize composition of functional gene categories according to hydrologic history, hydrologic treatment, plant presence/absence, and baseline (sampled before beginning hydrologic and plant treatments). We used permutational multivariate analysis of variance (PERMANOVA) to determine differences between bacterial communities among hydrologic history, hydrologic treatment, and plant presence. Hypothesis testing using PERMANOVA was performed using the *vegan::adonis* function (47). Unique taxa representing each hydrologic history and hydrologic treatment were determined by Dufrene-Legendre indicator species analysis using the *labdsv::indval* function (48). Finally, soil parameters were compared against bacterial community and functional patterns (based on

Bray-Curtis dissimilarity) using *vegan::envfit* function (47). Soil parameters with $p<0.05$ were represented on the PCoA plot of 16S rRNA community composition as vectors scaled by their correlation to microbial community patterns. The GHG concentrations with *envfit* $p<0.1$ were plotted as vectors, scaled by their correlation, on PCoA plots of functional gene composition.

We constructed linear mixed effects models with sampling plot and sampling date as random effects to determine the importance of the fixed effects of hydrologic history (field conditions), hydrologic treatment (contemporary dry/wet treatments), and plant presence on GHG concentrations using the *lme4* R package (49). Then, we used AICc model comparisons, which adjust for small sample size, against the null model to determine which simplest combination of fixed effects (hydrologic history, hydrologic treatment, and plant presence) is needed to explain the most variation in GHG concentrations (50, 51). We compared individual fixed effects and the combination of those fixed effects. We did not use the interaction between the fixed effects hydrologic history and hydrologic treatment because we only had a sample size of n=2 for each group. Lastly, to determine the proportion of variance explained by fixed effects (marginal) and the complete model (conditional), we used the *MuMIn* R package (51, 52). The CH_4, CO_2, and N_2O concentrations were log transformed to better meet normality assumptions prior to running mixed effects models. To assess microbial community structure and function relationships, we examined the relationship between individual GHG concentrations and microbial community/functional Bray-Curtis dissimilarity matrices using distance-based partial least squares regression in the *dbstats* R package (53). Finally, we used Mantel r statistic function in the *vegan* R package (47) to examine the relationship between the soil properties (redox, percent moisture, pH, ammonium, total soil C, phosphorus ppm, potassium ppm, magnesium ppm, sulfur ppm, and percent humic matter) and microbial community composition. Only soil properties with a correlation of <50% were used in this analysis.

Data Availability

All code and data used in this study are in a public GitHub repository (https://github.com/PeraltaLab/WetlandMesocosm_GHG_Timberlake), Raw amplicon sequence files can be found at NCBI SRA BioProject ID PRJNA636184, and metagenome sequence files can be found at NCBI SRA BioProject ID PRJNA641216.

Results

Characterization of soil physical-chemical properties

There was little variability in soil properties across main effects (hydrologic history, hydrologic treatment, plant presence). However, there were notable differences in soil moisture between plant treatments within dry and wet hydrologic treatments. In addition, NO_3^-N concentrations were below detection limits in samples with plants, but concentrations were measurable in samples without plants (0.01 ± 0.0005 to 0.25 ± 0.38 NO_3^-N mg L^{-1}) (Table 1). Soil redox status as measured by IRIS tube analysis revealed that soils experiencing dry and interim treatments (0% iron oxide paint removed) were not reducing, while soils in wet treatments were reducing (average 40%, range 27-67% paint removed). In wet treatments, plant presence decreased soil redox status to a lesser degree (average 38%, range 27%-60% paint removed) than when plants were absent, but soils were still considered reducing (Fig. 2, Fig. S1).

Plant and soil redox effects on greenhouse gas concentrations

Methane (CH_4) – Within no-plant treatments, wet (19.9 ± 42.0 mg CH_4-C m^{-2}, average ± SD) and interim (6.5 ± 25.4 mg CH_4-C m^{-2}) hydrologic treatments produced the highest CH_4 concentrations and the greatest variability between samples compared to dry treatments (0.22 ± 0.93) (Fig. 3A). However, treatments with plants produced the lowest CH_4 concentrations across wet, dry, and interim hydrologic treatments (0.64 ± 0.47, 0.17 ± 0.16, 0.60 ±0.85 mg CH_4-C m^{-2}, respectively) (Fig. 3A). The model with hydrologic history, hydrologic treatment, and plant

presence explained the most variation in CH_4 concentrations based on ΔAICc score of 0 and AICc weight of 0.45 (Table S1). The full model explained 32% of variation, while the fixed effect of hydrologic treatment explained 21% of the variation and plant and hydrologic history only explained 4% and 6%, respectively (Table S1).

Carbon dioxide (CO_2) – Within no-plant treatments, dry (104.7 ± 37.4 mg CO_2-C m^{-2}), interim (58.1 ± 30.6 mg CO_2-C m^{-2}), and wet (42.3 ± 18.5 mg CO_2-C m^{-2}) hydrologic treatments produced the highest CO_2 concentrations compared to treatments with plants (35.1 ± 19.2, 29.5 ± 15.0, 24.9 ± 0.6 mg CH_4-C m^{-2}, respectively) (Fig. 3B). The model with the interaction of hydrologic treatment and plant explained the most variation in CO_2 concentrations based on a ΔAICc score of 0 and AICc weight of 0.93 (Table S1). The fixed effect of plant explained 32% of the variation and hydrologic treatment explained 15% of variation while the interaction explained 52% of variation (Table S1).

Nitrous oxide (N_2O) – The N_2O concentrations were near zero in all hydrologic and plant treatments (range: 0.05-0.15 mg N_2O-N m^{-2}) (Fig. 3C). The model with hydrologic treatment and plant explained the most variation in N_2O concentrations based on ΔAICc score of 0 and AICc weight of 0.53 (Table S1). The full model explained only 14% of variation, while the fixed effect of plant explained 10% of variation and hydrologic treatment explained 3% of variation (Table S1).

Relationship between soil redox conditions and GHG concentrations

We used linear regression to examine the relationship between soil redox status and GHG concentrations. CH_4 had a weak but significant positive relationship to redox status (R^2=0.26, p=0.001) (Table S6). This relationship improved after removing a wet/no plant sample that had unusually high CH_4 concentrations (R^2=0.45, p<0.001) (Table S6). In addition, CO_2

concentrations had a weak but significant negative relationship with redox conditions (R^2=0.19, p=0.005), and N_2O concentrations were not significantly related to redox conditions (R^2=0.01, p=0.25) (Table S6).

Patterns in microbial community composition

Sequencing efforts returned a total of 1,570,135 reads and 35,897 operational taxonomic units (OTUs) before removing low abundance sequences occurring less than 10 times or 0.01% in all samples. After removing low abundance sequences, 1,505,797 reads representing 7,026 OTUs were retained after filtering. Within OTUs prior to filtering, 15,582 of those OTUs occurred once and 5,536 occurred twice in all samples. All samples were rarefied to 23,528 reads since this was the lowest read count among all samples.

Bacterial and archaeal community composition clustered by hydrologic treatment within hydrologic history (Fig. 4). The PCoA axis 1 explained 25% and PCoA axis 2 explained 11% of microbial community variation (Fig. 4). We observed that hydrologic history (PERMANOVA, R^2=0.305, p=0.001) and hydrologic treatment (PERMANOVA, R^2=0.110, p=0.002) explained variation in microbial community patterns (Fig. 4; Table S2). In contrast, microbial community composition was similar in the presence or absence of plant communities (PERMANOVA, R^2=0.102, p=0.824) (Table S2). In addition, sulfur concentrations were correlated to soil microbial communities from the wet hydrologic history, pH levels were correlated to microbial communities from the interim hydrologic history; and total soil C and manganese concentrations were correlated to microbial communities from the dry hydrologic history (Fig. 4). Also, overall patterns in microbial composition and soil properties were significantly correlated (Mantel r=0.32, p=0.001).

Indicator species analysis of the top 2.5% OTUs (by relative abundance at a significance level of p≤0.01) revealed that 34 OTUs, 21 OTUs, and 38 OTUs represented dry, interim, and wet hydrologic histories, respectively (Table S3, Table S4). The bacterial phyla Acidobacteria

(Gp1, Gp2, Gp3, and Gp6) (24%) and Proteobacteria (Alpha-, Beta-, Delta-, and Gammaproteobacteria) (30%) represented communities from dry hydrologic histories, while the bacterial phyla Acidobacteria (Gp1, Gp10, Gp3, and Gp7) (33%) and Proteobacteria (Alpha-, Beta-, and Deltaproteobacteria) (29%) represented communities from interim hydrologic histories (Table S4). Soils from wet hydrologic histories were represented by Acidobacteria (Gp1, Gp2, Gp3) (38%) and Proteobacteria (Alpha-, Delta-, and Gammaproteobacteria (21%) (Table S4). Finally, microbial taxa putatively associated with methane cycling including the archaeal genera *Methanobacterium* and the bacterial genera *Methylocystis* and *Syntrophobacter* were unique to microbial communities from wet hydrologic histories (Table S4). Fewer indicator OTUs were identified for hydrologic treatments (6 OTUs, and 9 OTUs, for interim, and wet hydrologic treatments, respectively) (Table S3). Only one indicator OTU was found in common among hydrologic histories and hydrologic treatments. Interestingly, this shared OTU, *Reyranella*, was indicative of both dry historical conditions, and wet hydrologic treatment conditions.

Patterns in functional gene composition

Following quality control and filtering of raw metagenomic sequencing data, annotation and gene calling resulted in 600,507 ± 172,049 (mean ± SD) annotated contigs per sample. An average of 998,604 ± 307,431 (mean ± SD) gene features per sample were identified. Of the identified gene features, an average of 232,809 ± 70,486 (mean ± SD) KEGG features per sample were identified. Among the four curated functional gene sets, central carbohydrate metabolism had the highest average KEGG features per sample (13,145 ± 3,848), followed by methanogenesis (1,434 ± 423), CcO (1,325 ± 398.26), and denitrification (350 ± 111).

The four functional gene categories (denitrification, methanogenesis, central carbohydrate metabolism, and CcO) showed varying responses to plant and hydrologic treatment but no response to interactions between plant and hydrologic treatments.

Carbohydrate metabolic composition differed between hydrologic treatment (PERMANOVA, R^2=0.09, P=0.04) but was similar across plant presence and absence (PERMANOVA, R^2=0.07, P=0.69) (Table S3). In contrast, the compositions of denitrification genes, methanogenesis genes, and CcO genes were similar across plant presence and hydrologic treatments (PERMANOVA, plant history: NS) (Table S3). Plant presence/absence had no significant impact on the composition of functional genes, which was also observed for 16S rRNA microbial community composition (Table S2, Table S3).

Based on environmental fitting (vegan::envfit), functional gene composition correlated to carbon losses (CO_2 and CH_4 production). Specifically, CO_2 concentrations correlated to the PCoA ordinations of functional gene composition associated with both denitrification (envfit, R^2=0.25, P=0.05) and carbohydrate metabolism (envfit, R^2=0.23, P=0.06) (Fig. 5), while the ordination of the methanogenesis genes had a marginally good fit with CH_4 production (envfit, R^2=0.20, P=0.09) (Fig. 5).

Relationships between GHG concentrations, microbial community composition, and soil properties

Microbial community composition explained more of the variation in GHG concentrations than do soil properties. Distance-based partial least squares regression revealed that microbial community composition explained 51.2%, 34.6%, and 38.0% (components 1 and 2), of variation in concentrations of CH_4, CO_2, and N_2O, respectively (Table 2). However, distance-based partial least squares regression revealed that patterns in soil properties only explained 30.0%, 31.6%, and 17.9%, of variation in concentrations of CH_4, CO_2, and N_2O, respectively, based on components 1 and 2 (Table 2).

We evaluated relationships among variation in GHG concentrations and variation in functional gene composition at the beginning ('start') and end of the experiment ('final') using distance-based partial least square regression. Denitrification gene composition explained

62.0% of variation in N_2O production at the start of the experiment, and 75.9% of variation in N_2O production at the end of the experiment (Table 2, components 1 and 2). Methanogenesis functional gene variation explained a higher proportion of CH_4 production in 'start' samples (67.6%) than 'final' samples (28.3%) (Table 2, components 1 and 2). 'Start' compositions of CcO and carbohydrate metabolism, explained 92.8% and 98.9% of variation in CO_2, respectively (Table 2, components 1 and 2). By the end of the experiment, CcO composition could only account for 4.39% of CO_2 production, while carbohydrate metabolism explained 77.0% of the variation in CO_2 production (Table 2, components 1 and 2).

Discussion

The presence of plants and dynamic hydrology interact to affect microbial community structure and function. This study revealed that initial hydrologic conditions (compared to manipulated hydrology) strongly influenced microbial community composition more than function. Specifically, results showed that hydrology is a strong environmental filter that determines microbial taxonomic and functional community patterns, short-term redox changes that are most distinct from historic redox conditions shift microbial communities, and plant presence can stabilize redox shifts and mediate greenhouse gas production.

Plant presence and dynamic hydrology influence greenhouse gas production to different degrees

Plant and hydrologic treatment strongly affected microbial function, despite hydrologic history acting as a robust environmental filter on microbial community composition. Plants can influence GHG rates by consuming CO_2 during photosynthesis, releasing CO_2 during respiration, aerating soils in contact with roots, and releasing labile C from roots which can stimulate microbial activity (18, 20, 54). In the current study, soil redox status as visualized with IRIS tubes indicated that oxidizing conditions existed near plant roots. This result suggested that

plants can transport oxygen belowground into soils. Regardless of hydrologic history, CH_4 concentrations were highest and CO_2 concentrations were lowest in soils experiencing the wet hydrologic treatment, while soil undergoing fluctuating hydrologic treatments had similar GHG concentrations to soils experiencing dry hydrologic treatments. As such, the GHG concentrations were lower in all hydrologic treatments with plants. Results suggest that oxygen radiation from plant roots could provide methanotrophs with needed oxygen for methane consumption, thereby decreasing methane emissions in the presence of plants (5, 18). The decline in CO_2 emissions in the presence of plants could be due to plant photosynthesis and plant uptake of atmospheric CO_2 from within the collection chamber (54). This study provides evidence that plants are important mediators of GHG production in wetland soils. Specifically, fluctuating soil moisture levels can decrease CH_4 emissions even when past environmental conditions reflect wet hydrologic histories. Therefore, both hydrology of soils and plant presence are important considerations when planning wetland restoration with the goal of enhancing soil carbon storage.

Past hydrology predicts bacterial community composition more than function

For this study, we collected wetland mesocosm soils from wet, dry, and interim hydrologic histories from a restored wetland. This change in hydrologic history resulted in different microbial community patterns with wet hydrology being the most distinct compared to microbial communities from the dry and interim hydrology. Specifically, dry hydrologic histories were represented by taxa in the genera *Gaiella*, which are classified as strict aerobes (55). Wet hydrologic histories were uniquely identified by bacterial and archaeal taxa putatively associated with methanogenesis, methanotrophy, and iron reduction. These microbial processes occur in low redox/low oxygen systems (6). Microbes that are facultative anaerobes can shift between aerobic and anaerobic respiration based on soil redox conditions, therefore they can metabolically shift during dynamic soil hydrologic conditions. However, obligate anaerobes such

as methanogens are sensitive to soil oxygen concentrations and desiccation (56). For example, in a study of peat bog layers, oxic subsurface layers contained more methanotrophs than methanogens which were found only in anoxic layers near the bottom of the bog (57). This suggests that hydrology is a strong determinant of oxygen availability in soils and that wet hydrologic histories best support microbial communities involved in anaerobic processes.

Mismatch between bacterial community composition and GHG function

The DNA-based functional gene composition explained variation in GHG concentrations measured at the beginning of the experiment more than at the end of the experiment. Hydrologic history influenced wetland soil microbial community composition more than contemporary treatments, which was emphasized in these results. The decrease in the strength of structure-function associations could be due to the DNA-based molecular measurement giving insight to historical and integrated environmental conditions and not contemporary changes to redox changes. Another explanation of decreased structure-function associations could be due to the differences in temporal resolution measured by DNA-based molecular methods compared to the *in situ* greenhouse gas measurements.

Functional gene composition predicts GHG concentrations to varying degrees

Cytochrome C Oxidase

To further examine microbial functional composition and measured GHGs, we subset the metagenomic data to focus on the composition of prokaryotic cytochrome C oxidase (CcO) genes as an indicator of aerobic respiration in more oxidizing redox conditions. While hydrologic history significantly influenced CcO composition (PERMANOVA, R^2=0.227, P=0.001, Table S3), CcO composition was unable to explain significant variations in GHG concentrations during the 8-week incubation (Table 2, Fig. 5). This lack of explanatory power is unsurprising, given the diversity of O_2-reducing terminal oxidases, and the known presence of CcO genes in strict

anaerobes (58, 59). There is no single enzyme that can be used to distinguish between aerobic and anaerobic phenotypes because aerobic and anaerobic organisms do not exist as binary groups (59). Instead, a spectrum of oxygen usage phenotypes exists (59). Evaluating the presence and number of a full suite of oxygen-utilizing enzymes may be a useful indicator of aerobic vs. anaerobic status (59), Therefore, bioinformatic methods to facilitate this method ought to be further developed.

Central Carbohydrate Metabolism

While CcO composition was unable to explain differences in CO_2 production across treatments, the composition of central carbohydrate metabolism genes was strongly related to differences in hydrologic history, hydrologic treatment, and the production of CO_2 (Table 2, Fig. 5, Table S3). In a past study, results revealed a significant positive correlation between carbohydrate-active enzyme abundance and cumulative respiration in a tundra soil warming experiment (60). Similarly, carbohydrate metabolism genes predicted differences in soil respiration between paddy and upland soils (61). While Johnston et al. did also find a relationship between CcO relative abundance and reducing conditions, this was the only study we could find that did successfully use CcO genes as an indicator of redox conditions. Johnston et al. also found the total relative abundance of carbohydrate active enzyme genes to be significantly positively related to cumulative ecosystem respiration (60). Liu et al. found several carbohydrate metabolism genes to be significant predictors of respiration rates in upland versus paddy soils (61). While there is no single gene or defined collection of genes that have been consistently used to explain microbial community respiration responses to redox changes, various collections of carbohydrate metabolism genes may reflect differences in soil redox status and respiration (60, 61).

Denitrification

When examining denitrifier community composition and greenhouse gas production, results showed that the composition of denitrification functional genes correlated to CO_2

concentrations but not N_2O concentrations (Fig. 5). The lack of association with N_2O is unsurprising since denitrifier community composition included the suite of genes involved in the reduction of nitrate to dinitrogen gas. The association between denitrification and CO_2 production is likely the result of organic denitrification, where organic matter is oxidized to CO_2 with nitrate as an electron acceptor (62). Organic denitrification, a form of respiratory denitrification, is typically a facultative process, found in organisms with the ability to respire aerobically when oxygen is available, and also use nitrate to respire anaerobically when oxygen availability decreases (63). A denitrification community-level response to soil hydrologic history and experimental drying/wetting has also been observed in a previous incubation experiment (64).

Methanogenesis

In the present study, we observed that hydrologic history (more than contemporary hydrologic treatment) influenced methanogenesis functional gene composition (Figs. 3 and 5, Table S3). Methanogenesis has historically been described as a specialized metabolism, in which methanogens are obligate anaerobes and obligate methanogens (meaning they do not use fermentation or alternative electron acceptors to grow) (65). While atypical methanogenic pathways have recently been discovered (e.g., aerobic bacterial methane synthesis) (66), classical anaerobic methanogenesis is still recognized as the primary source of biogenic methane production (65). In the present study, our results showed a strong influence of hydrologic history on methanogen functional gene composition, which supports the classical view of methanogenesis: a specialized and strictly anaerobic metabolism was maintained in the historically wet (i.e., low O_2) field conditions, and this history dictated mesocosms' methane production capacity. The structure-function analysis (based on dbplsr) provides another line of evidence that hydrologic history influenced methane production, where methanogen functional

gene composition explained a greater proportion of variation in CH_4 production at the start of the experiment, than at the end of the experiment (Table 2).

Considering plant-microbe relationships is critical to estimating wetland carbon storage potential

Our work highlights the importance of considering plant contributions to GHG emissions. Many studies investigating GHG emissions use opaque chambers to decrease heating of the headspace; however, these chambers can bias measurements of CH_4 emissions (54, 67). According to our study and others (54, 67), plant inclusion and plant species considerations in most cases would decrease the total estimation of CH_4 emissions from wetlands. These findings suggest that to improve estimations of C storage in wetlands, plant presence and hydrologic status should be considered to understand wetlands' potential to be a C sink.

Further, increasing extreme weather events cause changes in duration of decreased or excessive rainfall, which will alter microbial ecosystem functions. Changes in precipitation regimes could directly alter soil hydrology or plant abundance and composition. Results from this study revealed that the longer the duration of hydrologic change, the more dramatic the change in ecosystem functions. These results can be used to infer what might happen during an extreme drought event. One potential scenario is that during early summer a saturated non-tidal coastal plain wetland experiences decreased rainfall to the degree that the first meter of soil completely dries out and kills all vegetation. This may temporarily decrease methane emissions, but if in the following month the same area then becomes saturated again methane emissions could increase due to the lack of vegetation. However, if the duration of drying alters the microbial community structure, then methane production may be decreased upon re-flooding since obligate anaerobes will not persist under dry, aerated conditions. This warrants future studies to more closely examine the temporal component of hydrologic changes that permanently alter microbial community structure and lead to unexpected changes to ecosystem functions.

Acknowledgments

We thank J. LeCrone, L. Armstrong, M. Stillwagon, G. Gunderson, C. Eakins, J. Basco, and C. Bledsoe for field and laboratory assistance. We thank J. Gill and the East Carolina University grounds crew for their efforts in maintaining the grounds surrounding the shade house. We also thank M. Muscarella for microbiome analyses contributions. This work was supported by the National Science Foundation (Graduate Research Fellowship Program [GRFP] grant to R.B.B. and grant DEB #1845845 and CNH2 #2009185 to A.L.P.). The metagenomes were produced by the DOE JGI under the Community Science Program (CSP) (JGI CSP grant 503952). The work conducted by the DOE JGI, a DOE Office of Science User Facility, is supported under contract DE-AC02-05CH11231.

References

1. Kingsford RT, Basset A, Jackson L. 2016. Wetlands: conservation's poor cousins. Aquatic Conservation: Marine and Freshwater Ecosystems 26:892–916.
2. Fluet-Chouinard E, Stocker BD, Zhang Z, Malhotra A, Melton JR, Poulter B, Kaplan JO, Goldewijk KK, Siebert S, Minayeva T, Hugelius G, Joosten H, Barthelmes A, Prigent C, Aires F, Hoyt AM, Davidson N, Finlayson CM, Lehner B, Jackson RB, McIntyre PB. 2023. Extensive global wetland loss over the past three centuries. 7947. Nature 614:281–286.
3. Peralta AL, Stuart D, Kent AD, Lennon JT. 2014. A social-ecological framework for "micromanaging" microbial services. Frontiers in Ecology and the Environment 12:524–531.
4. Mitsch WJ, Bernal B, Nahlik AM, Mander Ü, Zhang L, Anderson CJ, Jørgensen SE, Brix H. 2013. Wetlands, carbon, and climate change. Landscape Ecology 28:583–597.
5. Truu M, Juhanson J, Truu J. 2009. Microbial biomass, activity and community composition in constructed wetlands. Science of The Total Environment 407:3958–3971.
6. Burgin AJ, Yang WH, Hamilton SK, Silver WL. 2011. Beyond carbon and nitrogen: how the microbial energy economy couples elemental cycles in diverse ecosystems. Frontiers in Ecology and the Environment 9:44–52.
7. Mentzer JL, Goodman RM, Balser TC. 2006. Microbial response over time to hydrologic and fertilization treatments in a simulated wet prairie. Plant and Soil 284:85–100.
8. Nygaard B, Ejrnæs R. 2009. The impact of hydrology and nutrients on species composition and richness: Evidence from a microcosm experiment. Wetlands 29:187–195.
9. Peralta AL, Ludmer S, Matthews JW, Kent AD. 2014. Bacterial community response to changes in soil redox potential along a moisture gradient in restored wetlands. Ecological Engineering 73:246–253.
10. Lennon JT, Jones SE. 2011. Microbial seed banks: The ecological and evolutionary implications of dormancy. Nature Reviews Microbiology 9:119–130.

718 11. Rocca JD, Hall EK, Lennon JT, Evans SE, Waldrop MP, Cotner JB, Nemergut DR,
719 Graham EB, Wallenstein MD. 2015. Relationships between protein-encoding gene
720 abundance and corresponding process are commonly assumed yet rarely observed. The
721 ISME journal 9:1693–9.
722 12. Kim SY, Lee SH, Freeman C, Fenner N, Kang H. 2008. Comparative analysis of soil
723 microbial communities and their responses to the short-term drought in bog, fen, and
724 riparian wetlands. Soil Biology and Biochemistry 40:2874–2880.
725 13. Mitsch WJ, Gosslink JG. 2007. Wetlands, 4th ed. John Wiley & Sons, Hoboken.
726 14. McDonald IR, Murrell JC. 1997. The Methanol Dehydrogenase Structural Gene mxaF and
727 Its Use as a Functional Gene Probe for Methanotrophs and Methylotrophs. FEMS
728 Microbiology Letters 156:205–210.
729 15. Conrad R. 2009. The global methane cycle: recent advances in understanding the
730 microbial processes involved. Environmental Microbiology Reports 1:285–292.
731 16. Kuzyakov Y. 2010. Soil Biology & Biochemistry Priming effects : Interactions between living
732 and dead organic matter. Soil Biology and Biochemistry 42:1363–1371.
733 17. Philippot L, Raaijmakers JM, Lemanceau P, Van Der Putten WH. 2013. Going back to the
734 roots: The microbial ecology of the rhizosphere. Nature Reviews Microbiology 11:789–799.
735 18. Chanton JP. 2005. The effect of gas transport on the isotope signature of methane in
736 wetlands. Organic Geochemistry 36:753–768.
737 19. Sundberg C, Jenny JS, Tonderski K, Lindgren PE. 2007. Overland flow systems for
738 treatment of landfill leachates-Potential nitrification and structure of the ammonia-oxidising
739 bacterial community during a growing season. Soil Biology and Biochemistry 39:127–138.
740 20. Carmichael MJ, Bernhardt ES, Bräuer SL, Smith WK. 2014. The role of vegetation in
741 methane flux to the atmosphere: should vegetation be included as a distinct category in the
742 global methane budget? Biogeochemistry 119:1–24.

21. Hu Q, Cai J, Yao B, Wu Q, Wang Y, Xu X. 2015. Plant-mediated methane and nitrous oxide fluxes from a carex meadow in Poyang Lake during drawdown periods. Plant and Soil https://doi.org/10.1007/s11104-015-2733-9.

22. Ardón M, Morse JL, Doyle MW, Bernhardt ES. 2010. The Water Quality Consequences of Restoring Wetland Hydrology to a Large Agricultural Watershed in the Southeastern Coastal Plain. Ecosystems 13:1060–1078.

23. Morse JL, Ardón M, Bernhardt ES. 2012. Greenhouse gas fluxes in southeastern U.S. coastal plain wetlands under contrasting land uses. Ecological Applications 22:264–280.

24. Ardón M, Morse JL, Colman BP, Bernhardt ES. 2013. Drought-induced saltwater incursion leads to increased wetland nitrogen export. Global Change Biology 19:2976–2985.

25. Hopfensperger KN, Burgin AJ, Schoepfer VA, Helton AM. 2014. Impacts of Saltwater Incursion on Plant Communities, Anaerobic Microbial Metabolism, and Resulting Relationships in a Restored Freshwater Wetland. Ecosystems 17:792–807.

26. Jenkinson BJ, Franzmeier DP. 2006. Development and Evaluation of Iron-Coated Tubes that Indicate Reduction in Soils. Soil Science Society of America Journal 70:183–191.

27. Rabenhorst MC. 2008. Protocol for Using and Interpreting IRIS Tubes. Soil Survey Horizons 49:74–77.

28. Schneider CA, Rasband WS, Eliceiri KW. 2012. NIH Image to ImageJ: 25 years of image analysis. Nature Methods 9:671–675.

29. Mehlich A. 1984. Mehlich 3 Soil Test Extractant: A Modification of Mehlich 2 Extractant. Communications in Soil Science and Plant Analysis 15:1409–1416.

30. Mylavarapu R, Obreza T, Morgan K, Hochmuth G, Nair V, Wright A. 2014. Extraction of Soil Nutrients Using Mehlich-3 Reagent for Acid-Mineral Soils of Florida. University of Florida Institute of Food and Agricultural Science 1–7.

767 31. Hoffmann M, Pehle N, Huth V, Jurisch N, Sommer M, Augustin J. 2018. A simple method
768 to assess the impact of sealing, headspace mixing and pressure vent on airtightness of
769 manually closed chambers. Journal of Plant Nutrition and Soil Science 181:36–40.
770 32. Millar N, Urrea A, Kahmark K, Shcherbak I, Robertson GP, Ortiz-Monasterio I. 2018.
771 Nitrous oxide (N2O) flux responds exponentially to nitrogen fertilizer in irrigated wheat in
772 the Yaqui Valley, Mexico. Agriculture, Ecosystems and Environment 261:125–132.
773 33. Caporaso JG, Lauber CL, Walters W a, Berg-Lyons D, Huntley J, Fierer N, Owens SM,
774 Betley J, Fraser L, Bauer M, Gormley N, Gilbert J a, Smith G, Knight R. 2012. Ultra-high-
775 throughput microbial community analysis on the Illumina HiSeq and MiSeq platforms. The
776 ISME Journal 6:1621–1624.
777 34. Apprill A, Mcnally S, Parsons R, Weber L. 2015. Minor revision to V4 region SSU rRNA
778 806R gene primer greatly increases detection of SAR11 bacterioplankton. Aquatic
779 Microbial Ecology 75:129–137.
780 35. Parada AE, Needham DM, Fuhrman JA. 2016. Every base matters: Assessing small
781 subunit rRNA primers for marine microbiomes with mock communities, time series and
782 global field samples. Environmental Microbiology 18:1403–1414.
783 36. Schloss PD, Westcott SL, Ryabin T, Hall JR, Hartmann M, Hollister EB, Lesniewski R a.,
784 Oakley BB, Parks DH, Robinson CJ, Sahl JW, Stres B, Thallinger GG, Van Horn DJ,
785 Weber CF. 2009. Introducing mothur: Open-source, platform-independent, community-
786 supported software for describing and comparing microbial communities. Applied and
787 Environmental Microbiology 75:7537–7541.
788 37. Kozich JJ, Westcott SL, Baxter NT, Highlander SK, Schloss PD. 2013. Development of a
789 dual-index sequencing strategy and curation pipeline for analyzing amplicon sequence
790 data on the miseq illumina sequencing platform. Applied and Environmental Microbiology
791 79:5112–5120.

792 38. Quast C, Pruesse E, Yilmaz P, Gerken J, Schweer T, Yarza P, Peplies J, Glöckner FO.
793 2013. The SILVA ribosomal RNA gene database project: Improved data processing and
794 web-based tools. Nucleic Acids Research 41:590–596.
795 39. Rognes T, Flouri T, Nichols B, Quince C, Mahé F. 2016. VSEARCH: a versatile open
796 source tool for metagenomics. PeerJ 4:e2584.
797 40. Schloss PD. 2021. Amplicon Sequence Variants Artificially Split Bacterial Genomes into
798 Separate Clusters. mSphere 6:e00191-21.
799 41. Glassman SI, Martiny JBH. 2018. Broadscale Ecological Patterns Are Robust to Use of
800 Exact Sequence Variants versus Operational Taxonomic Units. mSphere 3:e00148-18.
801 42. Peralta AL, Bledsoe RB, Muscarella ME, Huntemann M, Clum A, Foster B, Foster B, Roux
802 S, Palaniappan K, Varghese N, Mukherjee S, Reddy TBK, Daum C, Copeland A, Chen I-
803 MA, Ivanova NN, Kyrpides NC, Glavina del Rio T, Eloe-Fadrosh EA. 2020. Metagenomes
804 from Experimental Hydrologic Manipulation of Restored Coastal Plain Wetland Soils (Tyrell
805 County, North Carolina). Microbiol Resour Announc 9.
806 43. Chen I-MA, Markowitz VM, Chu K, Palaniappan K, Szeto E, Pillay M, Ratner A, Huang J,
807 Andersen E, Huntemann M, Varghese N, Hadjithomas M, Tennessen K, Nielsen T,
808 Ivanova NN, Kyrpides NC. 2017. IMG/M: integrated genome and metagenome
809 comparative data analysis system. Nucleic Acids Research 45:D507–D516.
810 44. Huntemann M, Ivanova NN, Mavromatis K, Tripp HJ, Paez-Espino D, Tennessen K,
811 Palaniappan K, Szeto E, Pillay M, Chen I-MA, Pati A, Nielsen T, Markowitz VM, Kyrpides
812 NC. 2016. The standard operating procedure of the DOE-JGI Metagenome Annotation
813 Pipeline (MAP v.4). Standards in Genomic Sciences 11:17.
814 45. Markowitz VM, Chen I-MA, Chu K, Szeto E, Palaniappan K, Pillay M, Ratner A, Huang J,
815 Pagani I, Tringe S, Huntemann M, Billis K, Varghese N, Tennessen K, Mavromatis K, Pati
816 A, Ivanova NN, Kyrpides NC. 2014. IMG/M 4 version of the integrated metagenome
817 comparative analysis system. Nucleic Acids Research 42:D568–D573.

46. R Core Team. 2019. R: A language and environment for statistical computing. R Foundation for Statistical Computing, Vienna, Austria.
47. Oksanen J. 2015. Vegan : ecological diversity 1:1–12.
48. Roberts D. 2016. Package ‘ labdsv .’ 1.8–0.
49. Bates D, Machler M, Bolker B, Walker S. 2015. Fitting Linear Mixed-Effects Models Using lme4. Journal of Statistical Software 67:1–48.
50. Hurvich C, Tsai C. 1993. A CORRECTED AKAIKE INFORMATIONON CRITERION FOR VECTOR AUTOREGRESSIVE MODEL SELECTION. Journal of Time Series Analysis 14:271–279.
51. Gorsky AL, Racanelli GA, Belvin AC, Chambers RM. 2019. Greenhouse gas flux from stormwater ponds in southeastern Virginia (USA). Anthropocene 28.
52. Barton K. 2019. Package “MuMIn.” R Package Version 1.43.15.
53. Boj E, Caballe A, Delicado P, Fortiana J. 2017. Package ‘ dbstats .’ R Package Version 1.0.5.
54. Luan J, Wu J. 2014. Gross photosynthesis explains the “artificial bias” of methane fluxes by static chamber (opaque versus transparent) at the hummocks in a boreal peatland. Environmental Research Letters 9.
55. Albuquerque L, França L, Rainey FA, Schumann P, Nobre MF, Da Costa MS. 2011. Gaiella occulta gen. nov., sp. nov., a novel representative of a deep branching phylogenetic lineage within the class Actinobacteria and proposal of Gaiellaceae fam. nov. and Gaiellales ord. nov. Systematic and Applied Microbiology 34:595–599.
56. Fetzer S, Bak F, Conrad R. 1993. Sensitivity of methanogenic bacteria from paddy soil to oxygen and desiccation. FEMS Microbiology Ecology 12:107–115.
57. Lew S, Glińska-Lewczuk K. 2018. Environmental controls on the abundance of methanotrophs and methanogens in peat bog lakes. Science of the Total Environment 645:1201–1211.

844 58. Esposti MD. 2020. On the evolution of cytochrome oxidases consuming oxygen.
845 Biochimica et Biophysica Acta (BBA) - Bioenergetics 1861:148304.
846 59. Jabłońska J, Tawfik DS. 2019. The number and type of oxygen-utilizing enzymes indicates
847 aerobic vs. anaerobic phenotype. Free Radical Biology and Medicine 140:84–92.
848 60. Johnston ER, Hatt JK, He Z, Wu L, Guo X, Luo Y, Schuur EAG, Tiedje JM, Zhou J,
849 Konstantinidis KT. 2019. Responses of tundra soil microbial communities to half a decade
850 of experimental warming at two critical depths. Proceedings of the National Academy of
851 Sciences 116:15096–15105.
852 61. Liu Y-R, Delgado-Baquerizo M, Yang Z, Feng J, Zhu J, Huang Q. 2020. Microbial
853 taxonomic and functional attributes consistently predict soil CO2 emissions across
854 contrasting croplands. Science of The Total Environment 702:134885.
855 62. Dlamini JC, Chadwick D, Hawkins JMB, Martinez J, Scholefield D, Ma Y, Cárdenas LM.
856 2020. Evaluating the potential of different carbon sources to promote denitrification. The
857 Journal of Agricultural Science 158:194–205.
858 63. Tiedje JM, Simkins S, Groffman PM. 1989. Perspectives on measurement of denitrification
859 in the field including recommended protocols for acetylene-based methods. Plant Soil
860 115:261–284.
861 64. Peralta AL, Ludmer S, Kent AD. 2013. Hydrologic history influences microbial community
862 composition and nitrogen cycling under experimental drying/wetting treatments. Soil
863 Biology and Biochemistry 66:29–37.
864 65. Lyu Z, Shao N, Akinyemi T, Whitman WB. 2018. Methanogenesis. Current Biology
865 28:R727–R732.
866 66. Wang Q, Alowaifeer A, Kerner P, Balasubramanian N, Patterson A, Christian W, Tarver A,
867 Dore JE, Hatzenpichler R, Bothner B, McDermott TR. 2021. Aerobic bacterial methane
868 synthesis. PNAS 118.

869 67. Günther A, Jurasinski G, Huth V, Glatzel S. 2014. Opaque closed chambers underestimate
870 methane fluxes of Phragmites australis (Cav.) Trin. ex Steud. Environmental Monitoring
871 and Assessment 186:2151–2158.
872
873

Figures and Tables

Figure 1

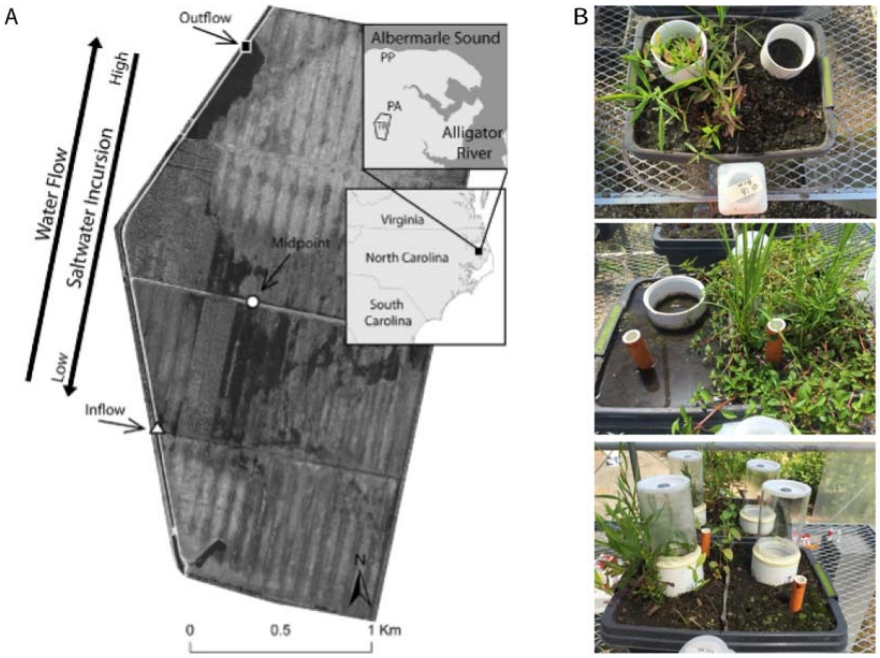

Figure 1. Field site and mesocosm set-up. Wetland mesocosms sourced from the Timberlake Observatory for Wetland Restoration (image modified from Ardón et al., 2013) (A). Aerial view of wetland mesocosm setup, where the left side of box represents plant treatment, and right side represents no plant treatment separated by a stainless mesh divider (B, top). PVC collars installed for measuring greenhouse gas concentrations. Also shown is a 1 liter bottle attached to each side of the mesocosm used to maintain water levels. Example of a wet treatment mesocosm with IRIS tubes installed (B, middle). Example of mesocosm with prepared for GHG sampling (B, bottom).

894 **Figure 2**

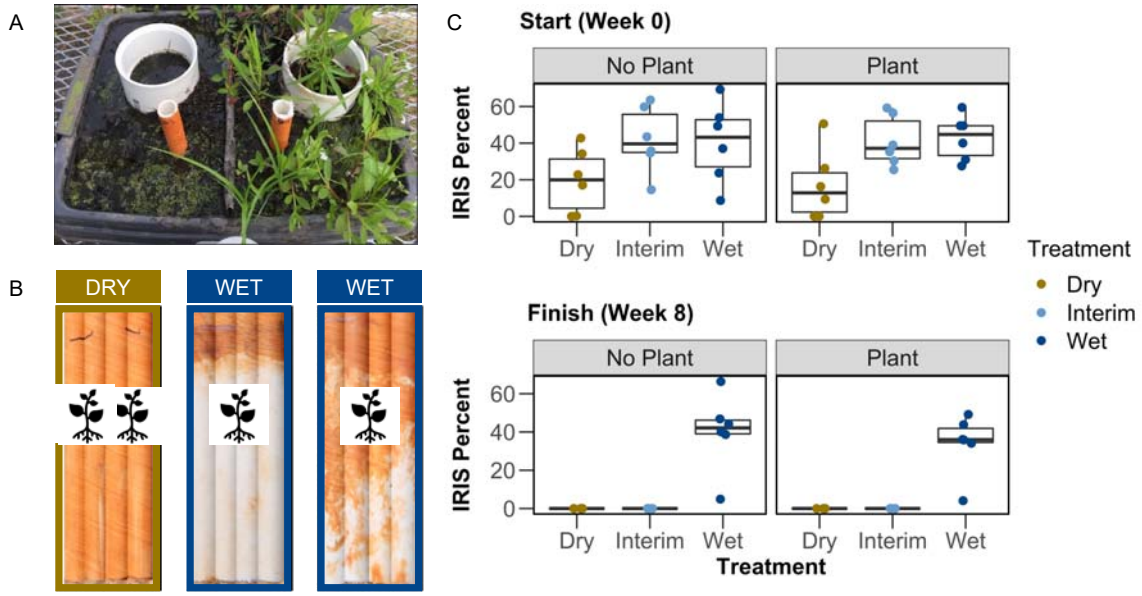

905

906 **Figure 2.** Indicator of reduction in soils (IRIS) tubes mesocosm image (A), IRIS tube example
907 image (B), and boxplots summarizing redox status at the beginning and end of experiment (C).
908 Percent paint removed from IRIS tubes at start of experiment (week 0) and the end of
909 experiment (week 8). Example IRIS tubes used for ImageJ analysis post-incubation (B) with
910 plant icons crossed out represent IRIS tubes from mesocosms with plants removed and plant
911 icons represent IRIS tubes from mesocosm with plants present. Box plots summarize percent
912 paint removed from IRIS tubes at start (week 0) and finish (week 8) of experimental incubation.
913 Individual samples are plotted as points and colored by hydrologic treatment.

914

915

Table 1. Soil chemical and physical properties measured after eight weeks of hydrologic manipulation. Average (mean ± standard deviation) by hydrologic treatment and plant status reported. Abbreviations: MDL = Below detection limit.

History Plant	Dry No Plant	 Plant	Interim No Plant	 Plant	Wet No Plant	 Plant
Moisture (%)	39 ± 0.31	14 ± 0.03	19 ± 0.16	13 ± 0.02	29 ± 0.23	62 ± 0.07
pH	5.31 ± 0.11	5.31 ± 0.09	5.4 ± 0.16	5.35 ± 0.1	5.55 ± 0.15	5.41 ± 0.17
NH_4^+ mg/L	0.39 ± 0.07	0.27 ± 0.04	0.26 ± 0.1	0.19 ± 0.02	0.77 ± 0.76	0.39 ± 0.42
NO_3^- mg/L	0.08 ± 0.07	MDL	0.25 ± 0.38	MDL	0.01 ± 0.0005	MDL
Total C (%)	4.63 ± 0.78	4.63 ± 0.81	4.48 ± 0.32	4.37 ± 0.52	4.91 ± 0.92	4.68 ± 0.74
Total N (%)	0.22 ± 0.03	0.22 ± 0.03	0.22 ± 0.01	0.21 ± 0.03	0.24 ± 0.04	0.23 ± 0.03
P ppm	21.00 ± 4.14	20.41 ± 4.4	23.58 ± 8.87	22.83 ± 8.37	23.16 ± 5.98	23 ± 5.79
K ppm	33.66 ± 5.97	30.25 ± 10.31	39.5 ± 11.44	26.75 ± 3.04	46.16 ± 16.02	34.25 ± 10.78
Mg ppm	77.58 ± 6.46	74.66 ± 11.43	86 ± 22.33	78.66 ± 16.47	89.25 ± 16.85	79.41 ± 18.8
S ppm	15.75 ± 1.94	15.33 ± 2.29	13.25 ± 1.25	12.16 ± 0.40	11.33 ± 1.21	11.5 ± 1.00
Fe ppm	252.66 ± 14.45	243.66 ± 17.06	275.33 ± 27.07	251.16 ± 37.6	306.83 ± 22.52	280.66 ± 40.71
Mn ppm	3.91 ± 1.15	3.41 ± 0.97	4.33 ± 1.16	4.58 ± 1.31	5.83 ± 1.32	5.58 ± 2.05
Humic matter (%)	2.35 ± 0.19	2.17 ± 0.14	2.04 ± 0.29	2.28 ± 0.22	1.98 ± 0.422	1.96 ± 0.43

932 **Table 2.** Summary of distance-based partial least squares regression (dbplsr) representing how much variation in GHG
933 concentration is explained (%) by each component (Comp) derived from functional gene composition, 16S rRNA gene composition,
934 or soil properties distance matrix.

GHG ~ Gene module or 16S rRNA or soils	Timepoint	Component	Comp 1	Comp 2	Comp 3	Comp 4	Comp 5	Comp 6
N_2O ~ Denitrification	Start	R^2	41.3	72.9	87.5	92.9	98.8	99.9
		adjusted R^2	31.6	62.0	78.2	83.4	95.7	99.5
		gvar	48.2	66.3	79.5	88.3	91.2	97.9
		crit	7.69e-5	4.84e-5	3.21e-5	2.86e-5	8.71e-6	1.43e-6
N_2O ~ Denitrification	Finish	R^2	76.2	79.1	82.9	86.6	91.0	94.1
		adjusted R^2	74.5	75.9	78.6	81.8	86.5	90.1
		gvar	9.09	44.0	64.9	83.3	87.4	91.3
		crit	1.98e-3	1.99e-3	1.89e-3	1.73e-3	1.39e-3	1.10e-3
CH_4 ~ Methanogenesis	Start	R^2	57.0	76.9	94.9	98.7	99.9	1.00e2
		adjusted R^2	49.9	67.6	91.1	97.0	99.6	99.7
		gvar	44.7	71.4	80.4	89.6	93.3	97.4
		crit	69.0	50.6	16.0	6.26	0.969	0.720
CH_4 ~ Methanogenesis	Finish	R^2	23.1	37.8	70.7	78.2	93.6	96.7
		adjusted R^2	17.7	28.3	63.4	70.2	90.4	94.6
		gvar	30.2	59.7	68.5	81.8	84.1	88.7
		crit	16.2	15.0	8.22	7.18	2.50	1.55
CO_2 ~ Central Carbohydrate Metabolism	Start	R^2	76.2	99.2	99.9	1.00e2	1.00e2	1.00e2
		adjusted R^2	72.3	98.9	99.8	1.00e2	1.00e2	1.00e2
		gvar	44.6	60.6	66.7	76.6	81.8	90.9
		crit	9.24	0.418	0.0956	0.0180	2.47e-4	1.19e-5
CO_2 ~ Central Carbohydrate Metabolism	Finish	R^2	44.1	80.1	85.5	92.0	98.1	99.6
		adjusted R^2	40.1	77.0	81.9	89.1	97.1	99.3
		gvar	22.4	28.4	62.4	76.0	80.6	84.4
		crit	25.1	10.3	8.67	5.62	1.60	0.433
CO_2 ~ Cytochrome C Oxidase	Start	R^2	49.3	94.8	97.8	99.6	99.8	1.00e2
		adjusted R^2	40.9	92.8	96.2	99.1	99.4	99.7
		gvar	75.1	87.9	96.6	97.4	98.8	99.4

		crit	19.7	2.73	1.64	0.459	0.392	0.211
CO_2 ~ Cytochrome C Oxidase	Finish	R^2	13.0	17.1	28.8	41.9	54.6	60.6
		adjusted R^2	6.78	4.39	11.0	20.8	31.9	34.3
		gvar	28.3	76.5	84.7	89.2	93.5	98.1
		crit	39.1	42.8	42.6	40.8	40.0	39.9
N_2O ~ 16S rRNA gene	Finish	R^2	27.4	41.6	71.3	87.8	92.9	97.0
		adjusted R^2	25.2	38.0	68.6	86.2	91.7	96.3
		gvar	10.1	36.8	49.4	56.9	66.4	71.2
		crit	1.58e-3	1.35e-3	7.04e-4	3.19e-4	1.98e-4	9.05e-5
CH_4 ~ 16S rRNA gene	Finish	R^2	22.6	54.0	82.2	94.1	96.8	99.4
		adjusted R^2	20.4	51.2	80.6	93.4	96.3	99.3
		gvar	28.3	44.3	52.3	57.8	65.9	69.1
		crit	3.10	1.96	0.802	0.281	0.163	0.0326
CO_2 ~ 16S rRNA gene	Finish	R^2	19.5	38.3	59.2	86.0	93.8	96.6
		adjusted R^2	17.1	34.6	55.4	84.2	92.8	95.9
		gvar	29.0	45.6	53.8	58.7	66.0	72.2
		crit	14.4	11.7	8.20	3.00	1.40	0.832
N_2O ~ soil parameters	Finish	R^2	12.2	22.6	28.6	42.7	54.0	65.5
		adjusted R^2	9.60	17.9	21.9	35.3	46.3	58.3
		gvar	37.0	63.8	73.4	77.2	81.6	84.5
		crit	1.92e-3	1.79e-3	1.75e-3	1.50e-3	1.28e-3	1.03e-3
CH_4 ~ soil parameters	Finish	R^2	13.3	34.0	64.2	76.7	92.8	96.5
		adjusted R^2	10.8	30.0	60.8	73.7	91.6	95.7
		gvar	49.6	65.4	70.6	76.5	78.8	81.4
		crit	3.48	2.81	1.62	1.12	0.369	0.194
CO_2 ~ soil parameters	Finish	R^2	12.5	35.5	45.5	51.6	58.2	66.5
		adjusted R^2	9.97	31.6	40.4	45.4	51.2	59.5
		gvar	52.6	60.1	64.5	72.1	80.5	84.8
		crit	15.6	12.2	11.0	10.4	9.53	8.16

Abbreviations are GHG, greenhouse gas; gvar, total weighted geometric variability; crit, value of criterion defined in method.

938 **Figure 3**

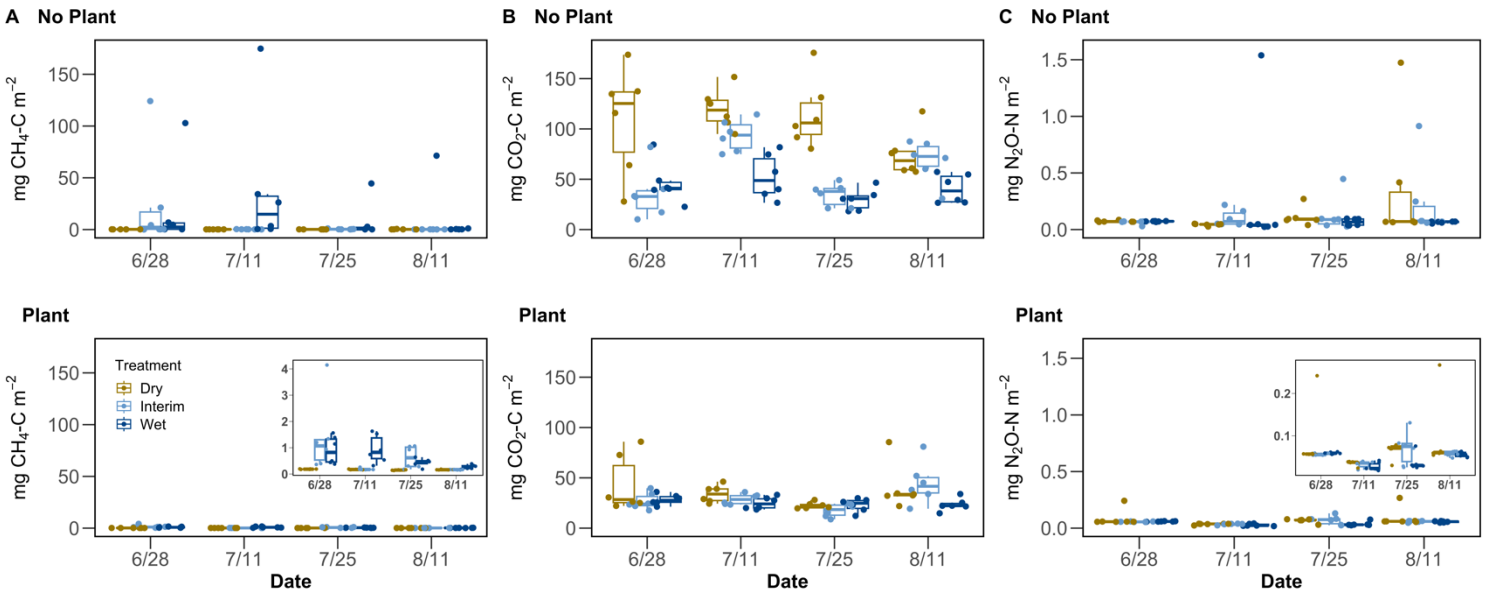

939

940 **Figure 3.** Boxplots of methane (CH_4) (A), carbon dioxide (CO_2) (B), and nitrous oxide (N_2O) (C) concentrations by hydrologic

941 treatment (Treatment), during four timepoints (Date). Samples from No Plant mesocosms are shown in the top panel, while samples

942 from mesocosms with plants are shown in the bottom panel. The insets in the bottom panels of (A) and (C) show zoomed in y-axis.

943 **Figure 4**

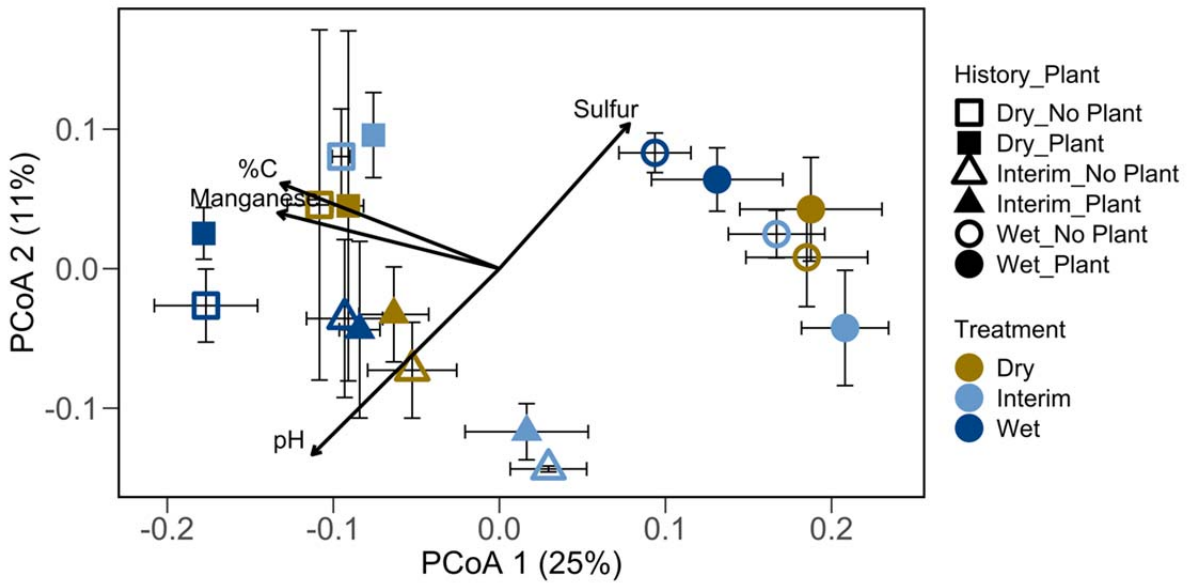

944

945 **Figure 4.** Ordination based on a principal coordinates analysis (PCoA) depicting community
946 composition of the bacterial and archaeal community composition based on the 16S rRNA
947 gene. Colors refer to hydrologic treatments: brown = dry, light blue = interim, dark blue = wet.
948 Shapes refer to hydrologic history of the sample: square = dry, triangle = interim, circle = wet.
949 Open shapes refer to samples from mesocosms without plants, while closed shapes refer to
950 samples from mesocosms with plants. Labelled vectors represent relationships among soil
951 physiochemical variables and the microbial community ordination with $P \leq 0.05$, scaled by their
952 correlation (using envfit).

953 **Figure 5**

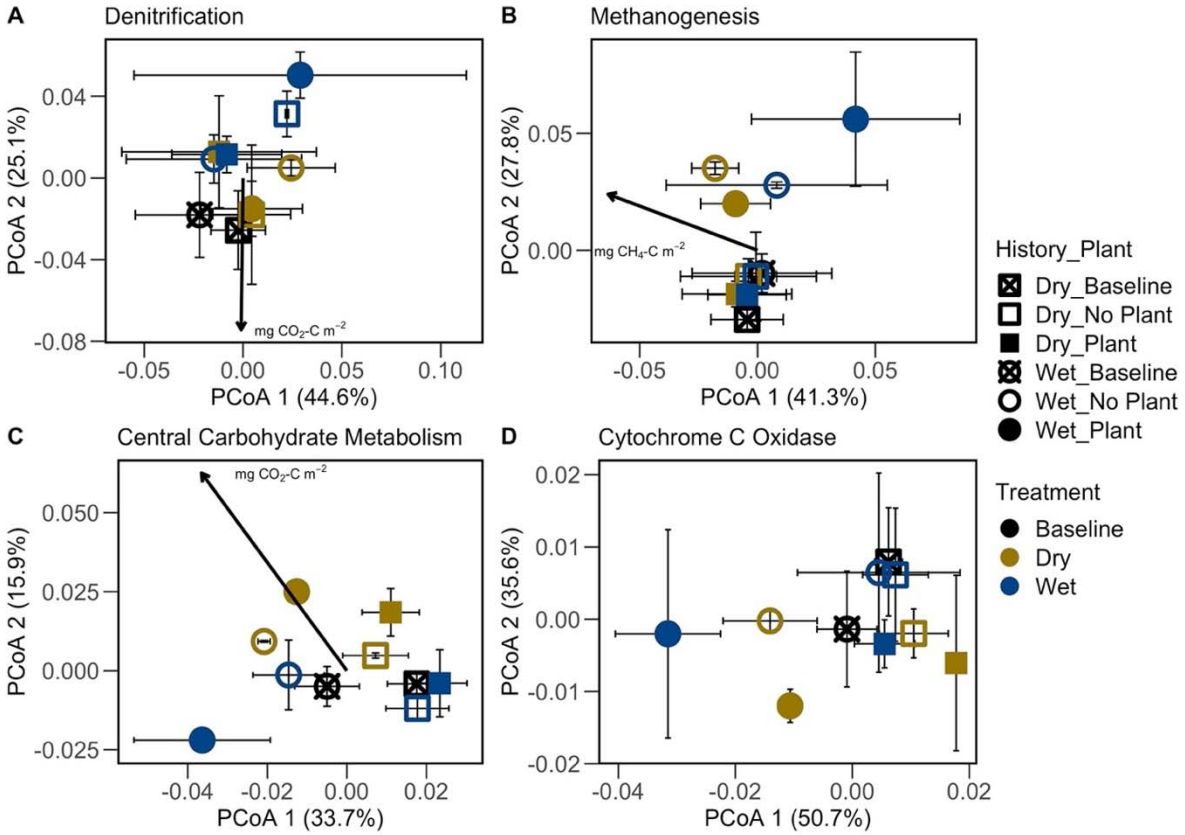

954

955 **Figure 5.** Ordination based on a principal coordinates analysis (PCoA) depicting community
956 composition of the functional gene modules. Panel A: Denitrification (KEGG Module M00529),
957 B: Methanogen (M00617), C: Central Carbohydrate Metabolism (M00001-M00011, M00307-
958 M00309, M00580, and M00633), D: Prokaryotic Cytochrome C Oxidase (M00155). Colors refer
959 to hydrologic treatments: black = baseline, brown = dry, dark blue = wet. Shapes refer to
960 hydrologic history of the sample: square = dry, triangle = interim, circle = wet. The shape fill
961 represents plant treatment: cross = baseline, open = no plant, closed = plant. Baseline samples
962 were collected before the start of hydrologic and plant treatments. Vectors represent significant
963 ($P \leq 0.1$) relationships among greenhouse gas trends and functional gene composition, scaled
964 by correlation (using envfit).

A

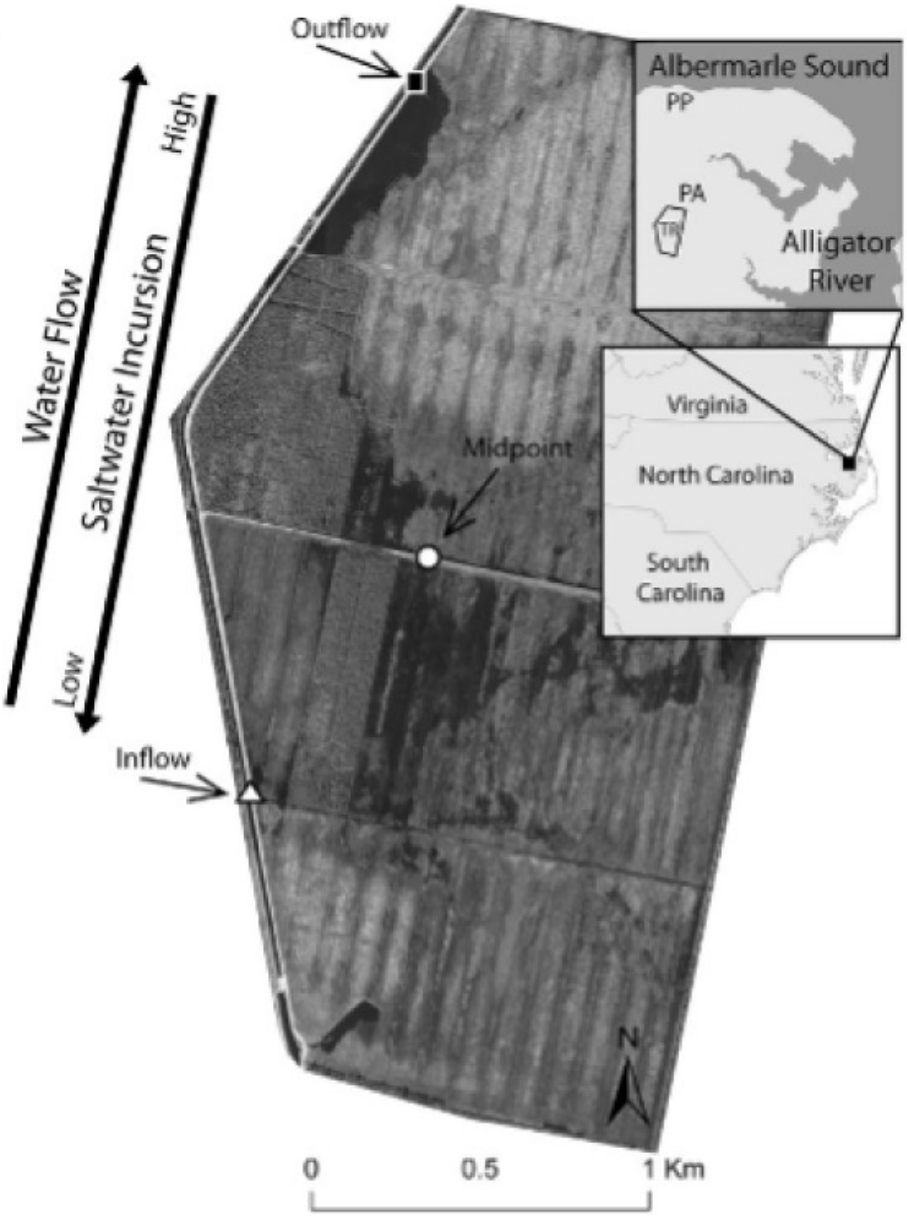
Outflow
Albermarle Sound
PP
PA
TR
Alligator River
Virginia
North Carolina
South Carolina
Water Flow
Saltwater Incursion
High
Low
Midpoint
Inflow
N
0
0.5
1 Km

B

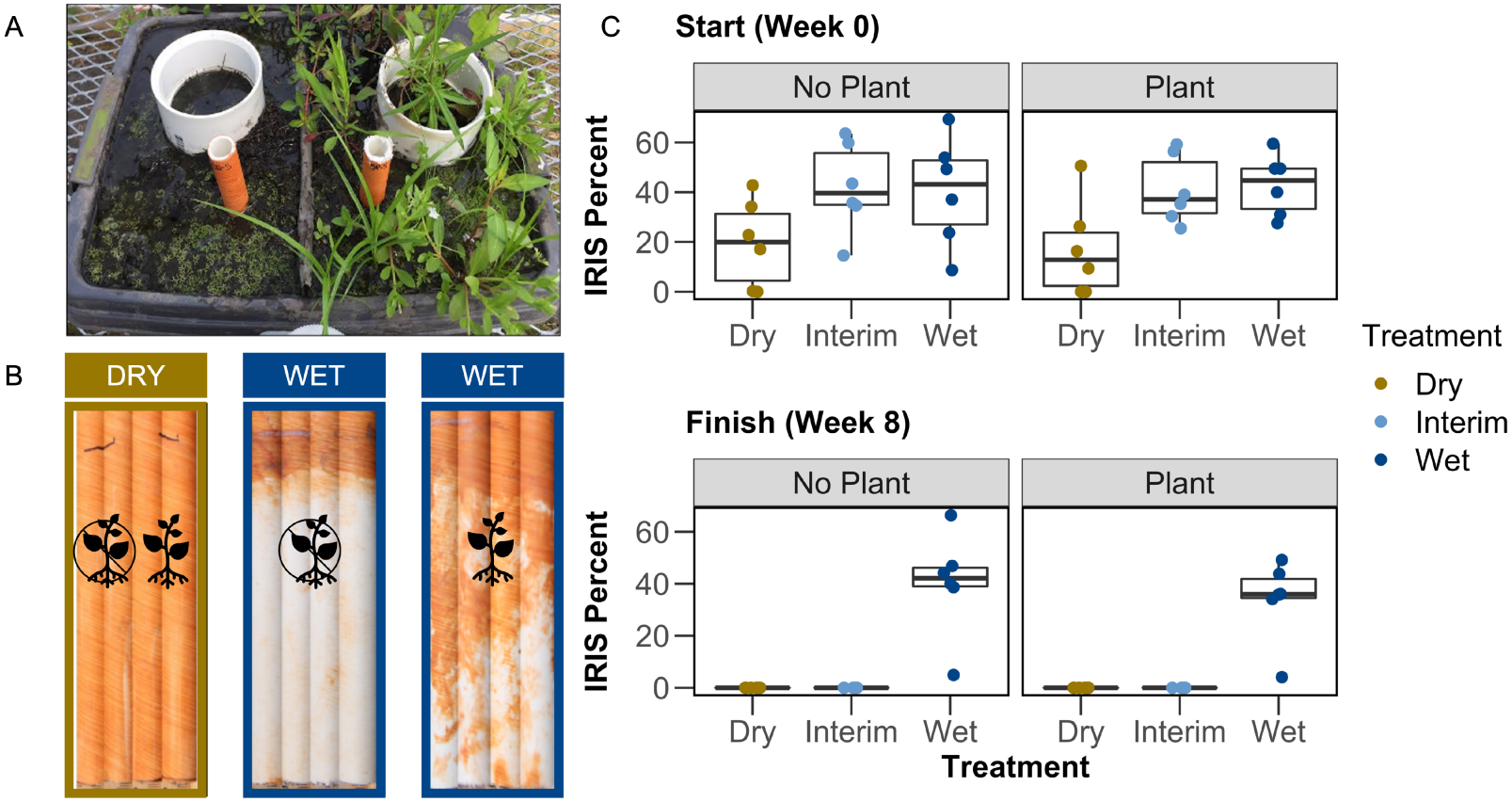
A
B
DRY
WET
WET
C
Start (Week 0)
No Plant
Plant
IRIS Percent
60
40
20
0
Dry
Interim
Wet
Finish (Week 8)
Treatment
Dry
Interim
Wet

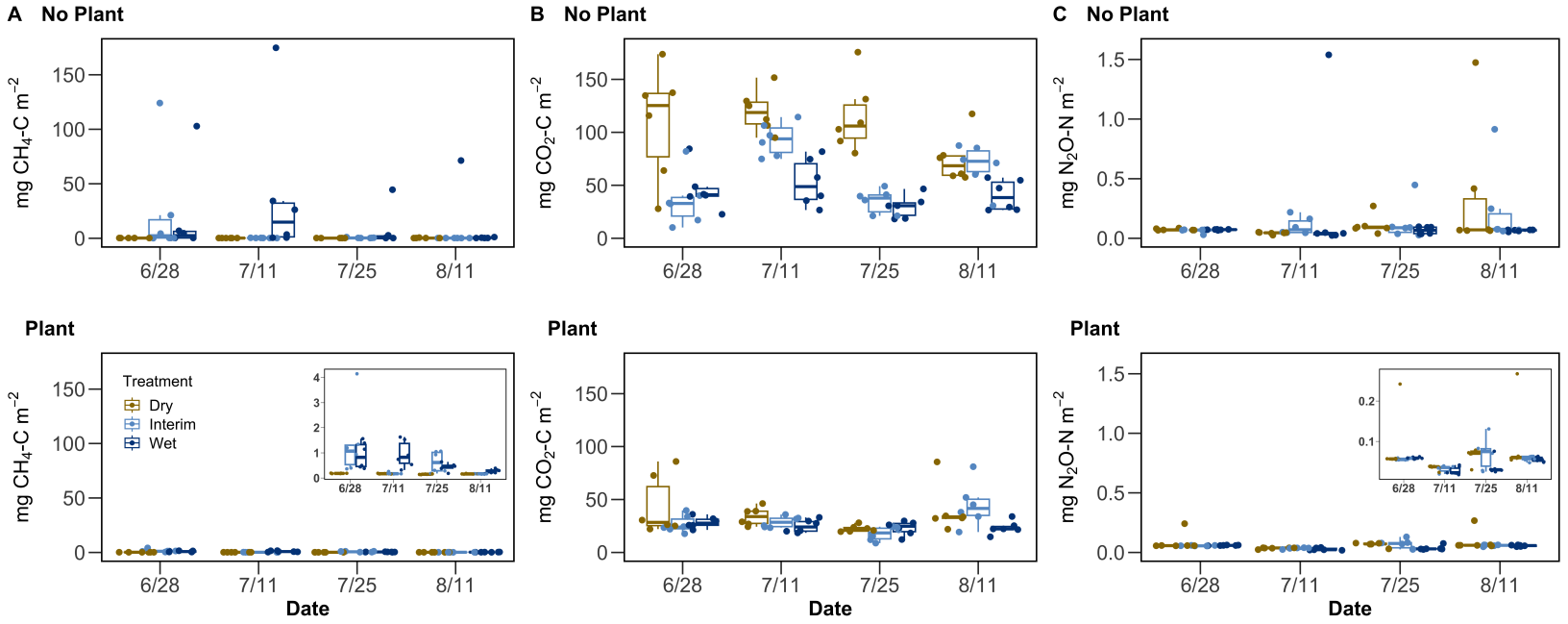
A No Plant
B No Plant
C No Plant
Plant
Plant
Plant
mg CH4-C m-2
mg CO2-C m-2
mg N2O-N m-2
Treatment
Dry
Interim
Wet
6/28
7/11
7/25
8/11
Date

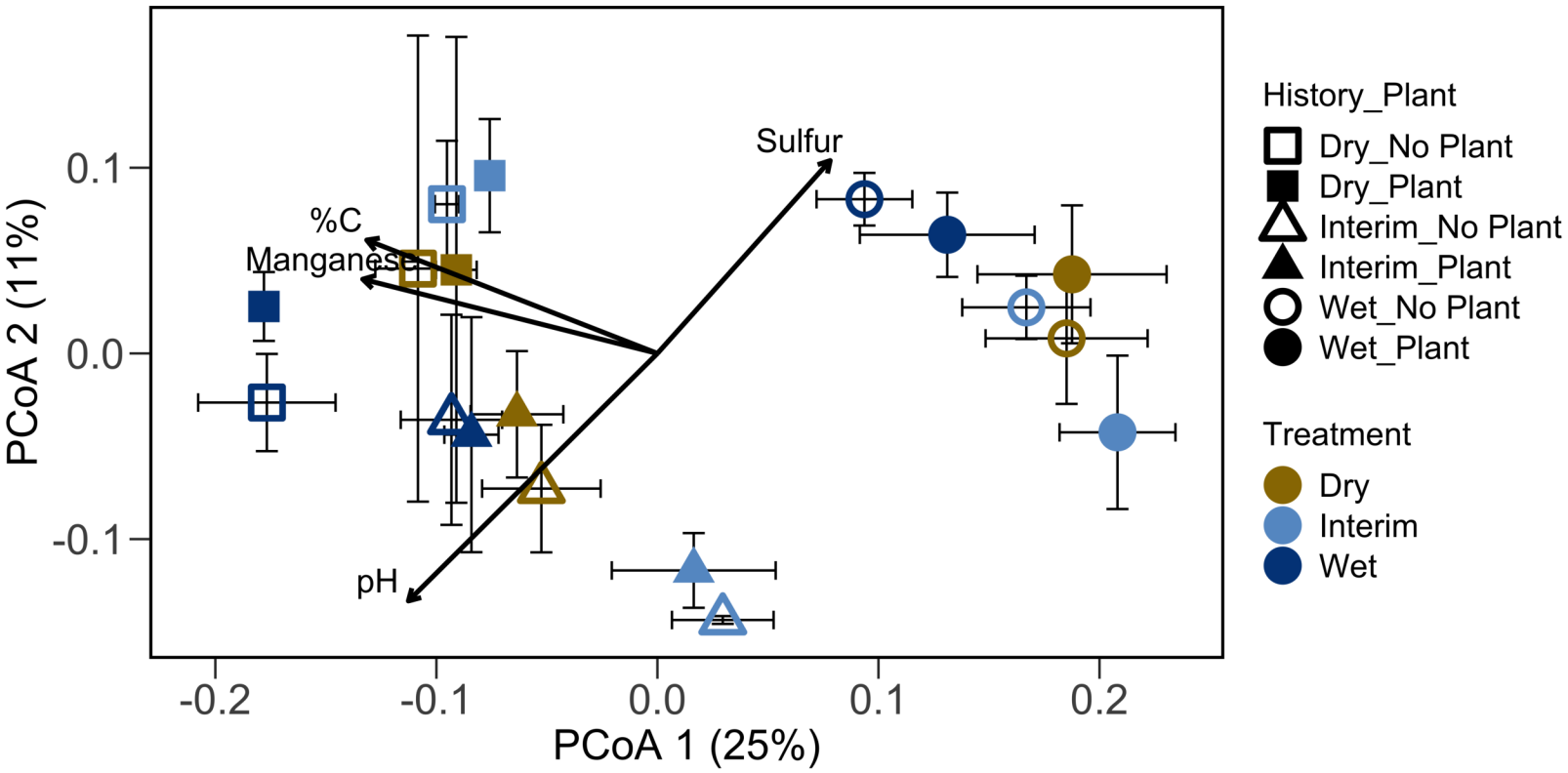
Sulfur
%C
Manganese
pH
0.1
0.0
-0.1
-0.2
-0.1
0.0
0.1
0.2
PCoA 2 (11%)
PCoA 1 (25%)
History_Plant
Dry_No Plant
Dry_Plant
Interim_No Plant
Interim_Plant
Wet_No Plant
Wet_Plant
Treatment
Dry
Interim
Wet

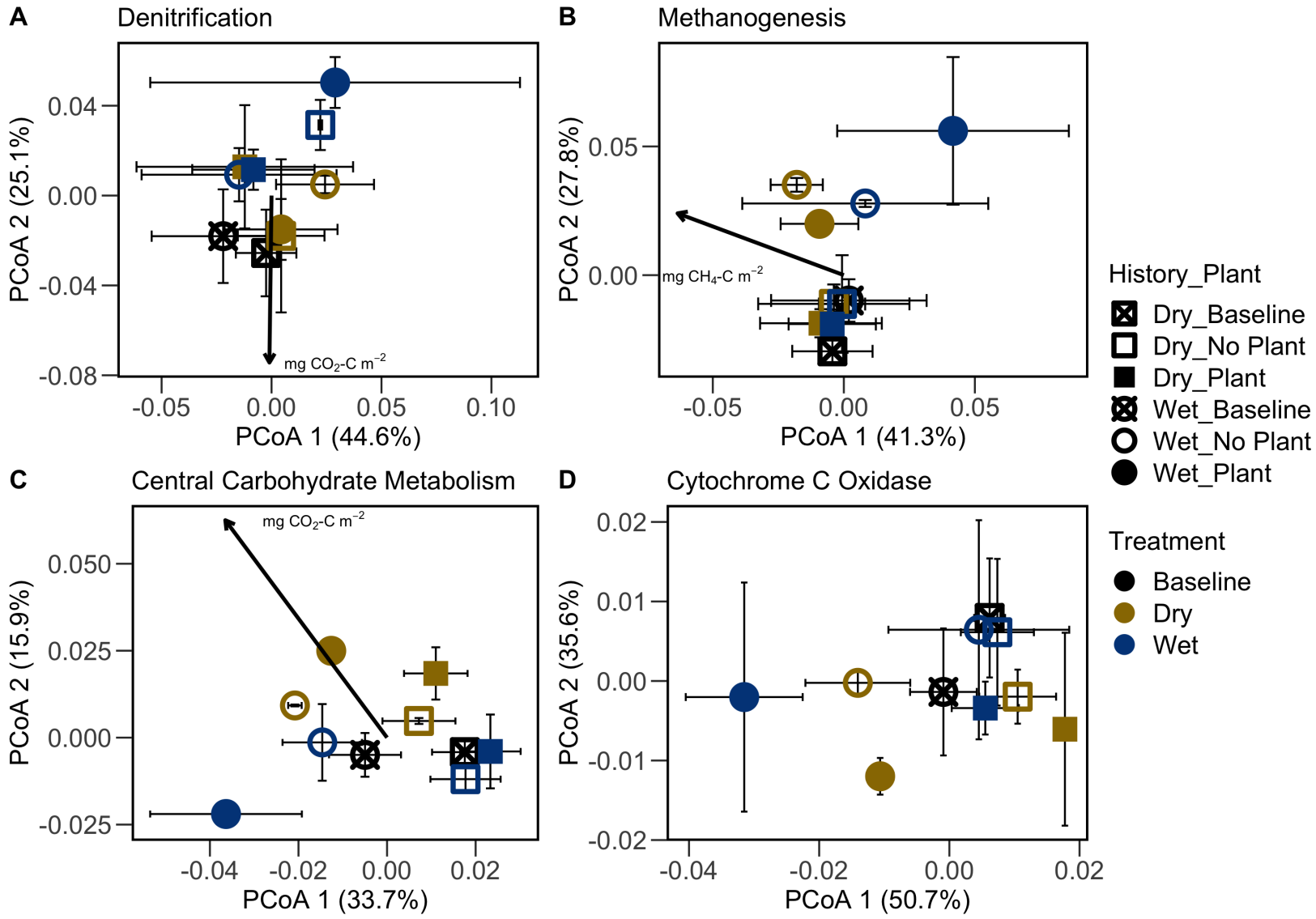
A
Denitrification
PCoA 2 (25.1%)
PCoA 1 (44.6%)
mg CO2-C m-2
B
Methanogenesis
PCoA 2 (27.8%)
PCoA 1 (41.3%)
mg CH4-C m-2
C
Central Carbohydrate Metabolism
PCoA 2 (15.9%)
PCoA 1 (33.7%)
mg CO2-C m-2
D
Cytochrome C Oxidase
PCoA 2 (35.6%)
PCoA 1 (50.7%)
History_Plant
Dry_Baseline
Dry_No Plant
Dry_Plant
Wet_Baseline
Wet_No Plant
Wet_Plant
Treatment
Baseline
Dry
Wet